Received: 1 February 2024 | Revised: 25 June 2024 | Accepted: 29 June 2024

DOI: 10.1111/bre.12886

Basin Research IAS EAGE WILEY

RESEARCH ARTICLE

Miocene sequences and depocentres in the Roer Valley Rift System

Alexandra Siebels[1,2] | Johan ten Veen[2] | Dirk Munsterman[2] | Jef Deckers[3] | Cornelis Kasse[1] | Ronald van Balen[1]

[1]VU University Amsterdam, Amsterdam, The Netherlands

[2]TNO (Geological Survey of The Netherlands), Utrecht, The Netherlands

[3]VITO (Flemish Institute for Technological Research), Mol, The Netherlands

Correspondence
Alexandra Siebels, VU University Amsterdam, Amsterdam, The Netherlands.
Email: alexandra_siebels@hotmail.com

Funding information
Geological Survey of the Netherlands (TNO-GDN)

Abstract

The Miocene sequence in the Roer Valley Rift System consists of alternating open-to-shallow marine, coastal and fluvio-deltaic deposits. In this study, well logs, biochronostratigraphy and seismostratigraphy are used to characterize major units and their bounding unconformities and to infer sediment dispersal patterns. Three major unconformities occur in the sequence: the early, middle and late Miocene unconformities (EMU, MMU and LMU). The EMU formed due to tectonic motions related to the Savian phase. After formation of the EMU, a broad depocentre developed in the south-eastern part of the Roer Valley Graben (RVG). Sediment accumulation increased during this period and peaked in the middle Langhian, after which it diminished again to a low level during the late Serravallian. The decrease in sediment accumulation coincided with a period of tectonic subsidence along the major bounding fault zones (i.e. the Peel Boundary Fault System, the Feldbiss Fault System and the Veldhoven Fault System). The resulting transgression caused sediment starvation in the central RVG. Subsequently, global sea-level fall during the early Tortonian caused large-scale erosion, and formation of incised valleys on the highs adjacent to the RVG (Peel Block and Campine Block), as well as the south-eastern RVG, forming the MMU. However, sedimentation continued during this period in the central part of the RVG where no erosional hiatus developed. From the Tortonian onwards, accumulation rates increased again. The depocentre shifted towards the north-west and clinoforms developed in the RVG. During the latest Miocene, the depocentre was concentrated along the south-western margin of the RVG. Meanwhile, the depositional environment of the entire RVRS gradually shallowed as the LMU was formed.

1 | INTRODUCTION

The Roer Valley Rift System (RVRS) is a tectonic entity located at the south-eastern margin of the Neogene North Sea Basin. Over the past decades, the Miocene sequence in the Roer Valley Rift System (RVRS) has been the subject of many studies. For the Belgian, or western part of the RVRS, the recent knowledge was compiled for the

lower-to-middle Miocene by Louwye et al. (2020) and the upper Miocene by Houthuys et al. (2020). The Dutch northern and eastern parts of the RVRS were covered by Munsterman et al. (2019). The German south-eastern part was studied over the years by Utescher et al. (2002), Schäfer et al. (2005), Prinz et al. (2016, 2017). All these studies focussed mainly on sedimentation on the shallower, less subsiding tectonic blocks at the margins of the RVRS, which are covered by plenty of boreholes or outcrops. The centre of the RVRS, the Roer Valley Graben (RVG), experienced stronger subsidence, and as a result is much less studied, as only few boreholes are drilled deep enough to reach the base of the Miocene sequence. Stronger subsidence resulted in more complete Miocene successions in the Roer Valley Graben (Munsterman et al., 2019). This makes the area key to linking the different sedimentation areas along the margins of the RVRS and getting a better understanding of its sedimentological evolution in the broader context of the tectonic and climatic forces that influenced the entire southern North Sea region.

The Miocene sequence was previously described in Dutch nomenclature as the upper part of the Veldhoven Formation and the Breda Formation. In a recent update of the stratigraphic framework proposed by Munsterman et al. (2019), it is suggested to subdivide the Breda Formation into an early-to-middle Miocene Groote Heide Formation and a late Miocene Diessen Formation (Figure 2). In this paper, a further specification of the lithostratigraphy and internal architecture in the RVRS is made. For this purpose, a multidisciplinary approach is used that combines well log analysis and biostratigraphy based on dinoflagellate cysts. We propose to further subdivide the Diessen Formation into four subunits, Diessen A–D. The stratigraphic architecture of the identified and characterized units and unconformities is determined using seismostratigraphy based on a network of old and new 2D seismic sections.

A better understanding of the mechanisms behind lateral and vertical sediment distribution as presented in this paper will aid in the future identification of suitable aquifers and aquitards, which is important for applications in geothermal energy and groundwater extraction.

Highlights

- This research includes the use of seismic data, well logs and dinocyst palynology.
- Results reveal a migration of the depocentre towards the north-west in the late Miocene.
- The Diessen Formation can be subdivided into four units that can be regionally correlated.
- The mid-Miocene unconformity has caused large incisions in the structural highs.
- No hiatus associated with the mid-Miocene unconformity is present in the central Roer Valley Graben.

2 | SETTING

2.1 | Structural background

The study area is located in the Roer Valley Rift System (RVRS), a NW–SE–trending rift basin that covers the southern part of the Netherlands, as well as parts of Belgium and Germany. The RVRS is bordered by the Rhenish Massif in the south and east, the Brabant Massif in the south-west and transitions into the North Sea Basin towards the north (Figure 1b). The adjacent Lower Rhine Graben forms the northern branch of the 1100-km-long European Cenozoic Rift System (ECRIS) (Geluk et al., 1994; Ziegler, 1990), the latter of which extends from the RVRS in the southern North Sea Basin, all the way to the Valencia Trough in north-eastern Spain (Zagwijn & Hager, 1987; Ziegler, 1990). The ECRIS formed in response to accommodate stress from the Alpine–Mediterranean orogenic system by northwards and southwards propagation from the Alpine foreland. The RVRS has undergone a complex late Palaeozoic-to-Cenozoic tectonic history, comprised of several phases of extension and inversion. The Miocene period is part of the final extensional phase that started in the late Oligocene and is still active to this day (Camelbeeck & Eck, 1994; Demyttenaere, 1989; Houtgast & van Balen, 2000; van Balen et al., 2002).

The Roer Valley Graben (RVG) forms the centre of the RVRS and is the focus area of this research. The RVG is bounded in the north-east by the Peel Boundary Fault System, and in the south-west by the Feldbiss Fault System, respectively, separating the RVG from the Peel Block and the Campine Block (Geluk et al., 1994). The Peel Block is bounded on the northern side by the Tegelen Fault System, which separates it from the Venlo Block (Figure 1a). The Roer Valley Graben transitions in the south-east to the tectonically interlinked Lower Rhine Basin (Michon et al., 2003; Sissingh, 2003).

In the RVRS, a regional hiatus developed during the late Oligocene that relates to the Savian tectonic phase (e.g. Dybkjær et al., 2021; Knox et al., 2010; Utescher et al., 2000; Verbeek et al., 2002; Ziegler, 1994). At the Oligocene–Miocene boundary, the direction of maximum extension changed from WNW-ESE to NE–SW and new depocentres developed from this renewed fault

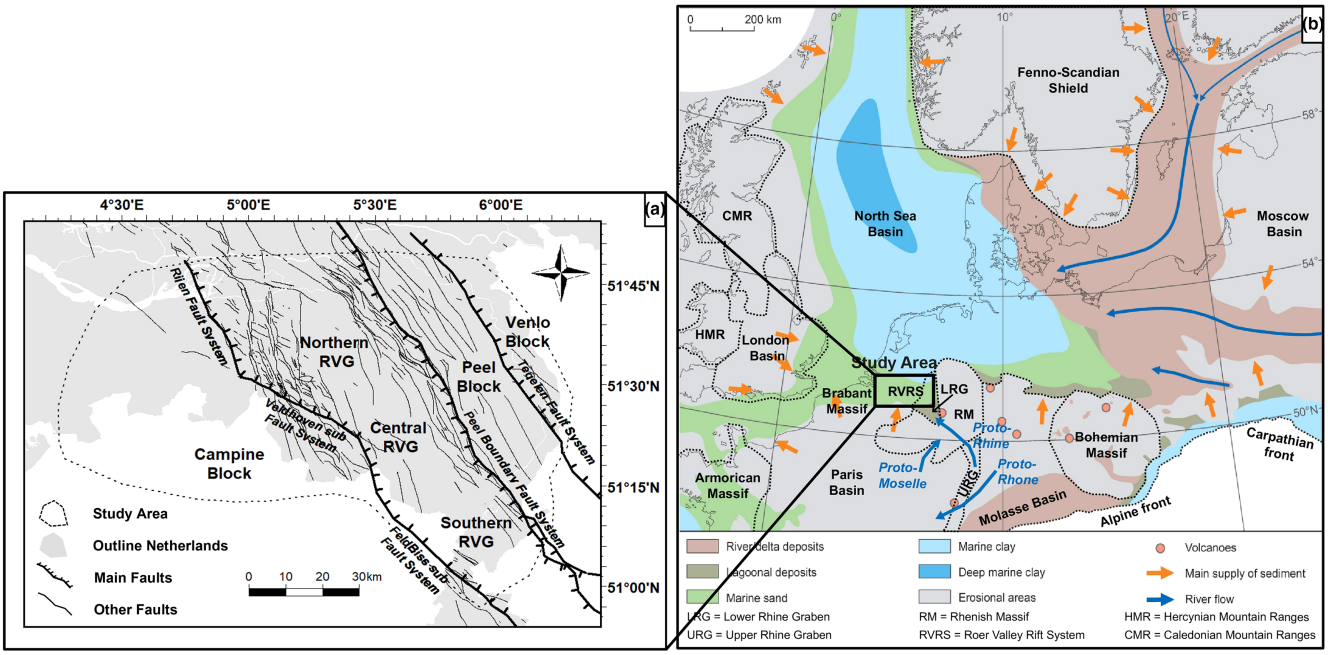

FIGURE 1 (a) Geological setting of the Roer Valley Rift System and (b) regional geological and palaeogeographical setting during the middle Miocene (modified after Böhme et al., 2012; Doornenbal & Stevenson, 2010; Gibbard & Lewin, 2003; Knox et al., 2010).

activity (Michon & van Balen, 2005). According to Geluk et al. (1994), the central RVG subsided a total of around 1000–1200 m since extension started in the late Oligocene, while the Peel Block experienced a maximum subsidence of 200 m during the same period. Correspondingly, the tectonic subsidence across the RVG varies between 250 and 600 m and between 30 and 110 m on the Peel Block (Michon et al., 2003).

2.2 | Sedimentological background

The late Oligocene start of rifting coincided with a sedimentological change from the Rupel Formation towards the Veldhoven Formation. The latter is composed of fine, glauconitic sands with some more silty/clayey intervals that were deposited from the Chattian up to the late Burdigalian (Figure 2). Sedimentation in the early Miocene starts with deposition of the Wintelre Member (Veldhoven Formation), consisting of lagoonal clay (Munsterman & Deckers, 2022). The Wintelre Member is transgressed and overlain by the marine, glauconite-rich sand of the Someren Member (Veldhoven Formation) during the late Aquitanian to middle Burdigalian. During the same time, its Belgian equivalent, the marine sand of the Berchem Formation, was deposited on the Campine Block, while in the Lower Rhine Basin, the marginal marine/continental sands of the German Köln Formation were formed (Figure 2).

The boundary between the Veldhoven Formation and Groote Heide Formation is the early Miocene unconformity (EMU) (Munsterman et al., 2019). The associated hiatus spanning the mid-Burdigalian–earliest Langhian is known in large parts of the North Sea Basin (Dybkjær et al., 2021; Munsterman & Brinkhuis, 2004; Utescher et al., 2000; Verbeek et al., 2002; Wong et al., 2001). In the Lower Rhine Basin, the EMU corresponds to a phase of regression that marks the expansion of the Morken II coal seam towards the north-west but is not reported as a hiatus here. On the Campine Block, this period coincides with the transition from the Belgian Edegem Member to the Kiel Member (Berchem Formation) and is represented by a hiatus in the late Burdigalian that developed in northern direction (Everaert et al., 2020) (Figure 2). The subsequent transgression coincides with the base of the Groote Heide Formation. In the north-western part of the Roer Valley Graben, the Groote Heide Formation consists of marine, glauconite-rich sands that were deposited during the Burdigalian–Serravallian. In the south-eastern part of the RVG, the Groote Heide Formation is differentiated into the Burdigalian marine glauconitic sands of the Kakert Member, the Langhian pale sands, including lignite seams of the Heksenberg Member and the Serravallian marine glauconitic sands of the Vrijherenberg Member (Munsterman et al., 2019). Further to the south-east, in the Lower Rhine Basin, extensive coastal swamps developed during this time, resulting in the formation of thick lignite accumulations of up to 100 m (Schäfer et al., 2005; Utescher et al., 2002). From

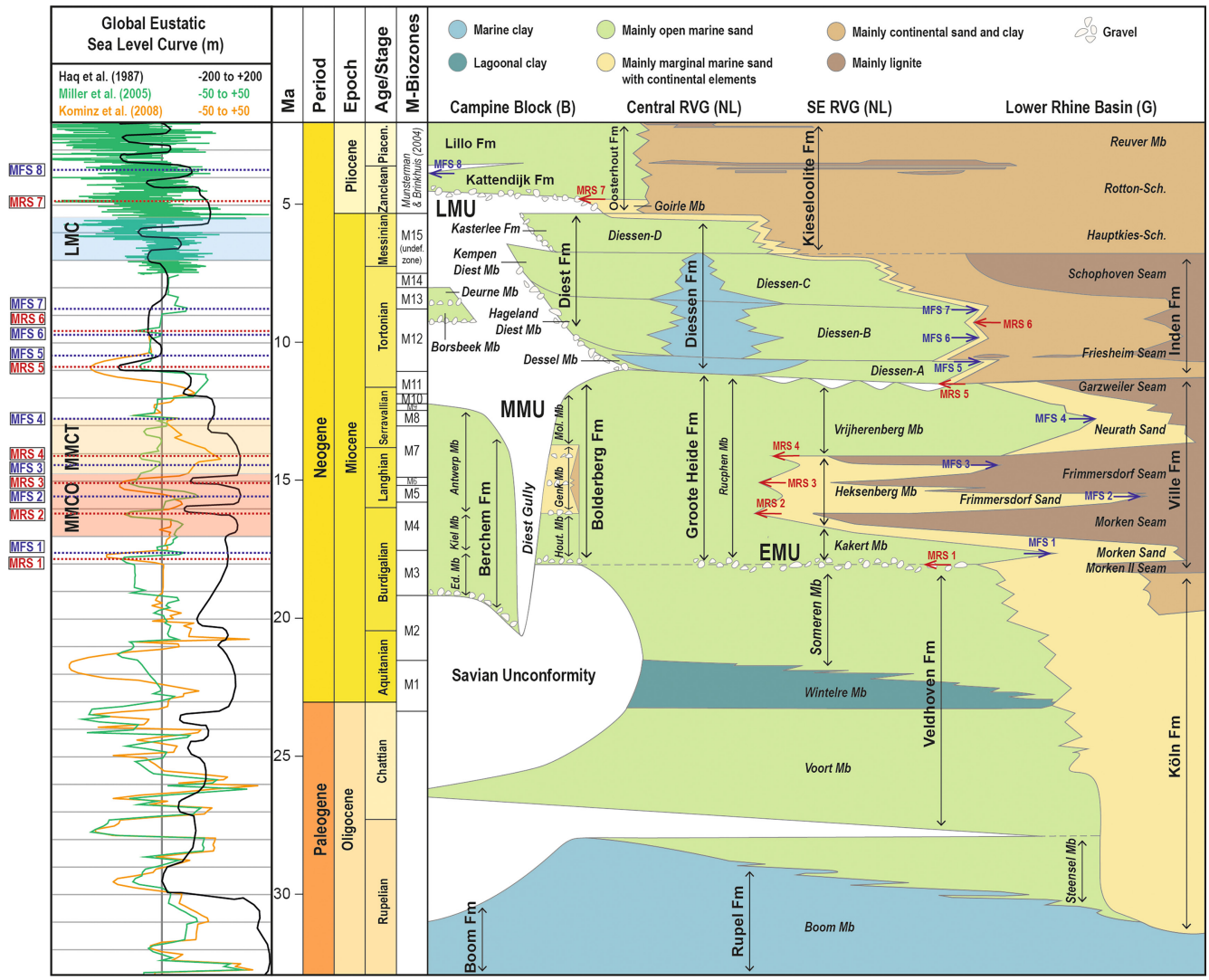

FIGURE 2 Schematic cross-section of the Miocene to early Pliocene lithostratigraphy and chronostratigraphy from the Campine Area (Belgium) to the Lower Rhine Basin (Germany). Modified after Van Adrichem Boogaert and Kouwe (1993), Deckers and Louwye (2019), Munsterman et al. (2019), Houthuys et al. (2020). Ed. Mb, Edegem Member; EMU, Early Miocene Unconformity; Fm, Formation; Hout. Mb, Houthalen Member; LMU, Late Miocene Unconformity; Mb, Member; MFS, Maximum Flooding Surface; MMU, Mid-Miocene Unconformity; Mol. Mb, Molenbeersel Member; MRS, Maximum Regressive Surface. Sea-level curves: Haq et al. (1987) (black); Miller et al. (2005) (green); and Kominz et al. (2008) (orange). MMCO, Mid-Miocene Climatic Optimum; MMCT, Mid-Miocene Climatic Transition; LMC, Late Miocene Cooling (Böhme, 2003; Flower & Kennett, 1994; Holbourn et al., 2013; Miller et al., 2020; Shevenell et al., 2008). Dinoflagellate cyst biozones after Munsterman and Brinkhuis (2004), calibrated to the timescale of Ogg et al. (2016) cf. Munsterman et al. (2019).

old to young these lignite seams are named the Morken, Frimmersdorf and Garzweiler seams. They are separated by sandy marine deposits of the Frimmersdorf Sand and Neurath Sand (Figure 2).

The boundary between the Groote Heide Formation and the Diessen Formation is the mid-Miocene unconformity (MMU) (Munsterman et al., 2019); a hiatus spanning the latest Serravalian–earliest Tortonian (Munsterman & Brinkhuis, 2004) because of the frequent absence of Biozone SNSM11. The timing and stratigraphic placement of the MMU in the wider North Sea Basin is variable. In the German Lower Rhine Graben, the MMU is pinpointed at the top of the Garzweiler Lignite Seam (Utescher et al., 2021), corresponding to an age of 13.8 Ma. Sørensen et al. (1997) also placed the MMU in the early Serravallian for the central and south-eastern North Sea areas, around 13.82 Ma. According to Goledowski et al. (2012), the MMU can be described as a condensed section in the North Sea Basin formed during the MMCO, which is followed by a transgression around 17–14 Ma. Huuse and

Clausen (2001), Huuse (2002), Eidvin and Rundberg (2007) and Rasmussen et al. (2008) correlate the MMU to the base of the Hodde transgression. In the eastern North Sea Basin, this surface corresponds to a distinct change from a prograding delta system with deposits consisting of shallow marine to continental sands and gravel to deposition of deeper marine mud (Rasmussen et al., 2010). The transgression is preceded by a regression and hiatus at the top of the Hordaland group that was recorded around 13 Ma. In contrast, the top of the Hordaland group is interpreted by Huuse and Clausen (2001) and Huuse (2002) as the MMU for the central Graben area where it represents a conformable downlap surface. Rasmussen and Dybkjær (2014) found in well located in the Danish offshore that the MMU rather represents a thin succession of around 3 m thick, beyond the seismic resolution, where sedimentation was continuous but little deposition took place over a timespan of several million years. Hence, during this 'MMU period', the stratigraphy is expressed differently throughout the North Sea Region. Overall, the MMU increased in duration westwards as the sediment supply was dominantly from the east, causing different age interpretations for the MMU. Although the transgression associated with the MMU may have been one of the largest during the Cenozoic, the MMU represents an unconformity in the western, British part of the southern North Sea Basin (Cameron et al., 1992). This is indicated by large-scale incision and absence of Miocene sediments, revealing an unconformity spanning the upper part of the Langhian and most of the Serravallian (11.6–14.8 Ma) (De Bruin et al., 2015).

The Diessen Formation consists of mainly open-to-shallow marine deposits with moderate-to-high glauconite content. Its strata are characterized by clinoforms, where foresets and toesets are preserved. Topsets are largely missing, which Munsterman et al. (2019) attribute to erosion during formation of the late Miocene unconformity (LMU). During the Pliocene, the prodeltaic depositional environment transitioned into a fluvial setting where gravel and sand of the Kieseloolite Formation were deposited (Meyer et al., 1983). This marked the onset of the proto-Rhine–Meuse River systems that continued to build out into the Roer Valley Graben. Böhme et al. (2012) showed

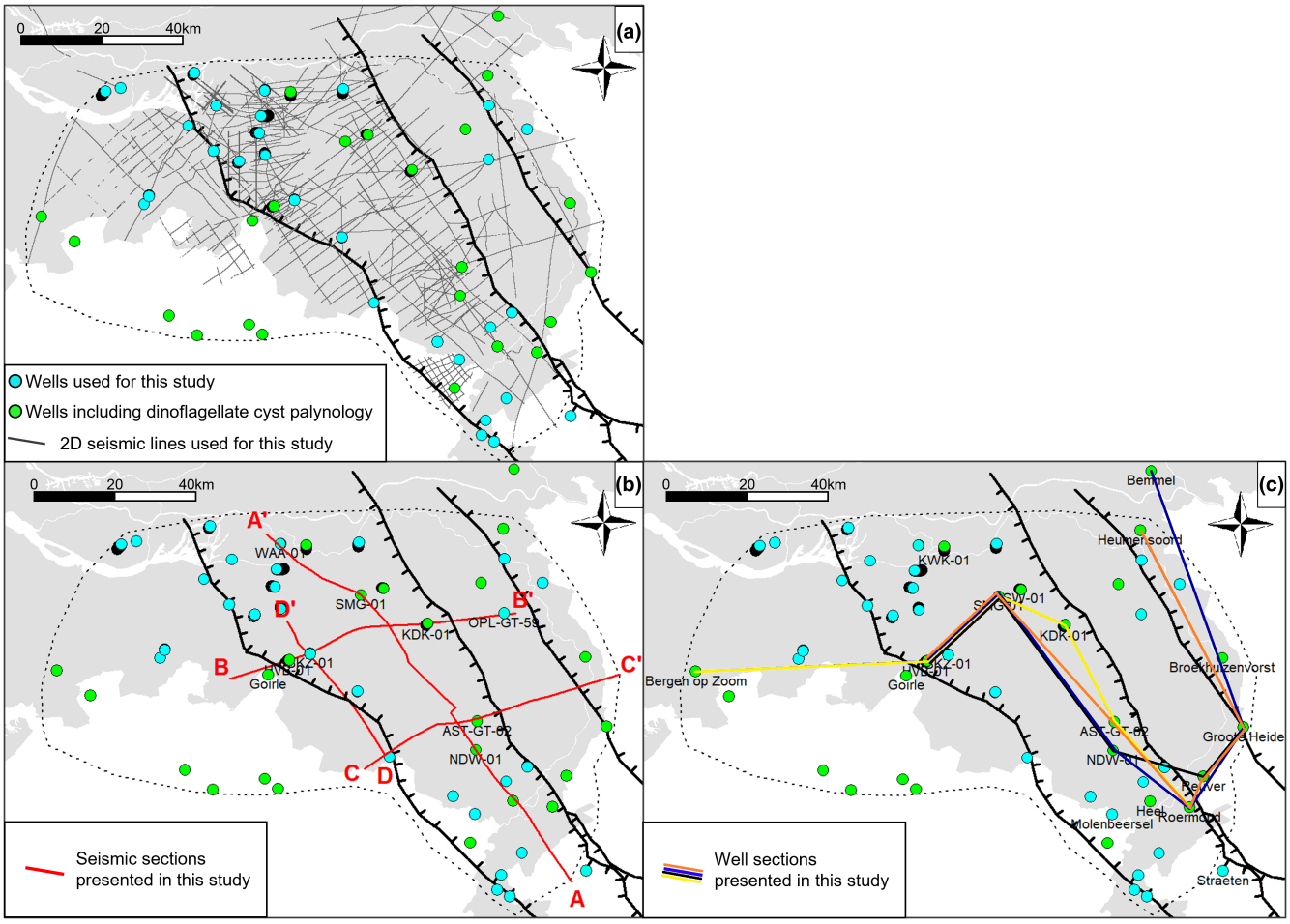

FIGURE 3 (a) Complete set of seismic lines (390) and wells (41) used in this study, (b) Location of the four (composite) seismic lines and some key wells and (c) Location of the four well log panels presented in this study, where black: Figure 4a, orange: Figure 4b, blue: Figure 4c and yellow: Figure 4d.

that the proto-Rhine reached the Lower Rhine Basin at the Miocene–Pliocene transition after it connected the river system in the Lower Rhine Basin with the proto-Rhine in the Upper Rhine Graben. The Rhine's connection to the Alps, however, was only established during the latest Pliocene, around 2 Ma (Boenigk & Frechen, 2006; Westerhoff et al., 2008). In the north-western part of the Roer Valley Graben, shell-rich sands of the Oosterhout Formation were deposited during the early Pliocene, as the distal equivalent of the Kieseloolite Formation (Munsterman et al., 2019; Slupik & Janse, 2008).

3 | DATA AND METHODS

3.1 | Well logs

The selected wells consist of 1 cored well, 15 air-lifted wells and 25 rotary-drilled wells (Figure 3). Dutch data were obtained from the NLOG and DINO loket portals (www.nlog.nl and www.dinoloket.nl), while Belgian well data were obtained from the DOV portal (www.DOV.vlaanderen.be).

Regional correlations were made using wireline logs and lithological descriptions of cores and cuttings. We also identified important sequence stratigraphic surfaces, such as maximum flooding surfaces (MFSs), following established methods (e.g. Catuneanu, 2006; Helland-Hansen & Hampson, 2009; Posamentier et al., 1988). Finally, correlation panels of key wells were constructed for four transects to investigate patterns between wells within the same chronostratigraphic units.

3.2 | Dinocyst palynology

Dinocyst palynology has significantly improved the age accuracy of the Miocene successions in the Roer Valley Rift System and NW Europe over the past decades (e.g. De Schepper et al., 2004; De Verteuil & Norris, 1996; Dybkjaer & Rasmussen, 2000; Louwye, 2002; Munsterman et al., 2019; Munsterman & Deckers, 2022). For this study, quantitative palynological analyses on dinoflagellate cysts are performed for 18 wells (Figure 3b). From this selection, 13 wells were analysed by TNO (Geological Survey of the Netherlands), and 5 boreholes were previously analysed by Louwye (1999, 2005). Palynological reports of Dutch 'deep' wells are available on the NLOG portal. The others (e.g. air-lifted wells) are available on request via the DINO loket portal.

The zonation scheme used for this study is derived from Munsterman and Brinkhuis (2004), who identify 14 Miocene 'Biozones' (SNSM1 to SNSM14, or M1 to M14 in short). All zones are updated to the GTS2016 timescale of Ogg et al. (2016) in Munsterman et al. (2019). We also introduce an additional zone here, defined as Biozone SNSM15 (M15), representing the latest Tortonian–Messinian (Figure 2). This was an unzoned interval in Munsterman and Brinkhuis (2004). The boundaries of a certain Biozone are determined using a combination of chronostratigraphical last (youngest) occurrences (LODs) and first (oldest) occurrences (FODs) of certain dinoflagellate cyst species. The use of only LODs is performed to exclude the possibility of caving (collapse of borehole walls). The sampling density varies per well, depending on the nature of the material (cuttings vs. airlifted samples) and the purpose of the analysis (e.g. selection of strategic sample locations). Rotary-drilled wells commonly have low sampling resolutions due to the extended depth intervals (cost factor).

3.3 | Seismic data and interpretation

Seismic reflection data consist of 390 2D seismic lines (Figure 3b) of varying quality and vintages that were collected over the past 60 years, mostly for hydrocarbon exploration. Among these, 10 high-resolution seismic lines were acquired since 2019 by the SCAN project (Seismische Campagne Aardwarmte Nederland = Dutch Seismic Campaign for Geothermal Energy), where focus was put on depths between 500 and 4000 metres, aligning with the scope of this study. All seismic lines are accessible through the data portal of NLOG.

The sampling rate for SCAN lines is 2 ms TWT, while older seismic surveys are sampled at 4 ms TWT. Assuming an average velocity of 1800 m/s, and an observed dominant frequency in the top 1500 m of 60–90 Hz (at a 2 ms sampling rate) and 30–45 Hz (at a 4 ms sampling rate), this corresponds to a vertical resolution of approximately 5–7.5 m and 10–15 m respectively. The data are processed in reverse (European) polarity using a zero-phase wavelet, where a hard kick represents a negative (blue) reflection (trough) and a soft kick represents a positive (red) reflection (peak).

A seismic-to-well ties study was conducted to facilitate comparison and calibration of seismic data with well log data. Convolution of the reflection coefficient series with a wavelet was constituted to create synthetic seismograms that model the seismic response of the subsurface. The reflection coefficient series hereby represents contrasts in acoustic impedance between different geological layers that can be calculated using the sonic logs (and density logs, if available). A wavelet is then chosen based on the frequency characteristics of the seismic survey at a targeted interval. The logs are then convoluted with this

TABLE 1 Seismic and well log characteristics of the early Miocene unconformity (EMU), mid-Miocene unconformity (MMU) and late Miocene unconformity (LMU) used to regionally correlate these surfaces throughout the research area.

	Reflection characteristics	Gamma-ray and sonic log signatures		Example seismic cross-section
LMU	Low-amplitude, medium-frequency reflector, picked on a peak. Truncation surface for underlying clinoform foresets of the Diessen Formation and onlap surface for overlying clinoforms of the Oosterhout Formation in the north-western RVG. Less evident towards the south-east, where reflectors run parallel but sometimes small incisions are observed.	The LMU is marked on top of a gamma-ray peak, followed by a low gamma-ray sequence on top in the deeper parts of the RVRS. In the shallower parts, the LMU is marked at the top of a coarsening-upward sequence, followed by a spikey gamma-ray log pattern. The sonic log displays a dip in slowness just below the LMU.	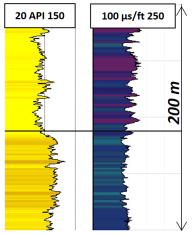	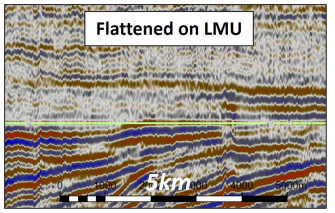
MMU	Medium-amplitude, variable-frequency reflector, picked on a peak. Represents a truncation surface below the MMU towards the rims of the RVG, as well as a downlap surface above. The MMU often marks the basal part of large-scale prograding clinoforms. On the Peel Block and in the south-eastern RVG, large incised valleys are observed (45–95 m) below the surface of the MMU.	In the deeper parts of the RVRS, the MMU is marked just above a peak in the gamma-ray signal and is recognized by a transition from higher to lower values in the upward direction. In the shallower parts, the MMU is positioned at the top of a coarsening-upwards sequence followed by a short fining-upward sequence. The sonic log generally displays distinctive peaks in slowness just above the MMU; in other wells, the MMU is located at a sharp dip in slowness.	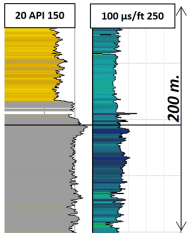	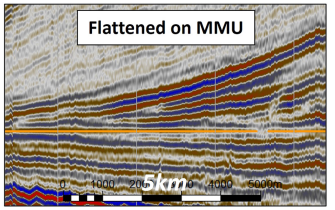
EMU	High-amplitude, high-frequency reflector, picked on a peak. Represents a low-angle truncation surface below the EMU and a low-angle onlap surface above. Not visible everywhere. Reflections often run parallel above and below the EMU.	The EMU is difficult to recognize in the deeper RVRS (figure displayed here) but is often marked at the base of a short fining-upward sequence in the shallower RVRS. The sonic log displays a dip in slowness at the EMU.	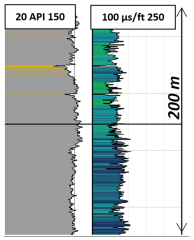	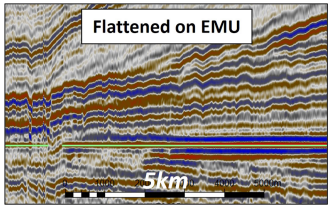

Note: Gamma-ray logs are derived from well SMG-01 (Figure 3a). Seismic windows are extracted from SCAN line 17 + 18 (section B–B′ on Figures 3a and 7).

seismic wavelet to generate a synthetic seismic response that is in correspondence with the resolution of the real seismic data. A Ricker wavelet was applied here, using a representative frequency that matches the dominant frequency of the seismic data in the concerned depth interval. Time–depth relationships were determined using sonic logs and, when available, in combination with check shot data. Petrel© v2020.4 software was used to perform well log correlations, seismic-to-well ties and seismic interpretations.

Seismic reflection data are utilized to interpret (1) stratigraphic units, (2) unconformities and (3) sequence stratigraphic surfaces. A primary focus was put on the main intra-Miocene unconformities (EMU, MMU and LMU) (Table 1). Identification of the lithological units is aided by seismic facies, which are defined by reflection characteristics, such as amplitude, frequency, geometry and continuity (Table 2). Well log patterns, lithological descriptions and palynological records are correlated to seismic features to determine their stratigraphic position and infer lateral changes in depositional environments (e.g. Harding, 2015; Patruno et al., 2015). Major transgression and regression events are most clearly recognized by reflector terminations, adhering to the principles of sequence stratigraphy (Catuneanu, 2006). These sequence stratigraphic horizons are typically bounded by clinothems: sets of genetically related clinoforms. Their geometry is crucial for sequence stratigraphy and basin infill analysis (Steel et al., 2003). Each clinoform can be regarded as an increment of time in which sediment is deposited. They provide information on key changes in progradation direction, relative sea level, basin accommodation and sediment supply (Hampson et al., 2009; Helland-Hansen & Hampson, 2009; Helland-Hansen & Martinsen, 1996). Clinoform trajectories are mapped on 2D seismic sections, where the rollover points from topset to foreset are connected. These trajectories function as progradation vectors. By performing this exercise on multiple seismic lines, a pseudo-3D progradation direction is obtained. Seismic cross-correlations ensure a correct correlation between clinothems of the same system. Trajectories are grouped in seismic subunits Diessen-A, -B, -C and -D (Figure 10).

4 | RESULTS

The Miocene sequence in the south-eastern Netherlands is subdivided into five formations (Figure 2). These units are based on the stratigraphic framework of Munsterman et al. (2019), but more detail is added to the late Miocene Diessen Formation, which is further divided into four subunits. Below, we first characterize the units using borehole information (logs, descriptions and biostratigraphy) and illustrated well log panels (Figure 4). In the second part, we characterize the stratigraphic architecture using seismostratigraphy (Tables 1 and 2, Figures 5–8). The location of the wells and well log panel sections are indicated on Figure 3.

4.1 | Well log correlations and biostratigraphy

4.1.1 | Veldhoven Formation

The Chattian (late Oligocene) to Aquitanian–Burdigalian (early Miocene) Veldhoven Formation is composed of three members, namely the Voort, Someren and Wintelre members (Figure 2). The unit is composed of shallow marine (<200 m depth) deposits consisting of clays and sands. On the Peel Block and Venlo Block, the Veldhoven Formation mainly exists of sands, making it difficult to distinguish between the Voort and Someren members (TNO-GDN, 2024), whereas in the Roer Valley Graben, the clay-rich Wintelre Member is situated in between. Thickness variations across faults and structural entities are common as the formation was deposited during rifting (Deckers, 2016; Munsterman et al., 2019).

4.1.1.1 | *Voort Member*

The late Oligocene (Chattian) Voort Member is composed of stacked coarsening upwards successions that can be tens of metres thick (Figure 4a). The sand is generally fine-grained, grey-green and glauconitic, where a middle neritic-to-littoral marine environment is interpreted (TNO-GDN, 2024). The member consistently overlies the Steensel Member of the Rupel Formation (Deckers & Munsterman, 2020). The transition between the Steensel Member and Voort Member is often marked by an upward increase in glauconite content. In general, well log characteristics for the Voort Member show a variable gamma-ray log pattern, but two subtle bell shapes can be distinguished in wells SMG-01, NDW-01 and Reuver (Figure 4a). The gamma-ray log pattern here suggests two coarsening-upwards and fining-upwards successions, where the base of the Voort Member is marked by a coarsening-upwards succession and the top by a fining-upwards succession. SP log values in wells Reuver and Groote Heide are high and tend to decrease towards the top. A slight gradual increase in resistivity is observed towards the top as well. Corresponding borehole descriptions from well Groote Heide confirm a decrease in the clay content towards the top of the Voort Member. The more variable gamma-ray pattern may be explained by a variable abundance in marine glauconite.

TABLE 2 Properties of seismic facies encountered in the seismic units of the Miocene sequence.

Seismic facies	Occurrence	Reflection characteristics and geometry	Example seismic cross-section (Height = 0.2 s, width = 6 km) 20× vertical exaggeration
SF1 Fluvial	Kiezeloolite Fm.	• Variable amplitude, variable frequency • Contorted/hummocky/chaotic, discontinuous • Conform to underlying topography • Incised channels	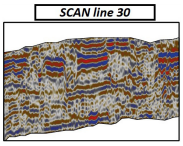
SF2 Shoreface Clinoforms	Oosterhout Fm.	• Very variable amplitude and frequency • Limited continuity • Oblique-tangential clinoforms • Onlap and downlap the underlying topography, toplap against the overlying topography	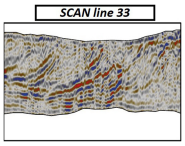
SF3 Intrashelf Clinoforms	Diessen Fm.	• Variable amplitude, high frequency • Limited continuity • Oblique and sigmoidal clinoforms • Onlap and downlap the underlying topography, and either toplap or offlap the overlying topography	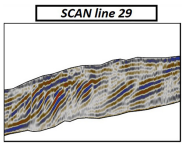
SF4 Shelf-Edge Clinoforms (Background Facies)	Diessen Fm.	• Low amplitude, low frequency • Continuous reflectors • Sigmoid clinoforms • Internal low-angle onlap and truncation features, drape underlying topography (MMU) in the central part of the RVG	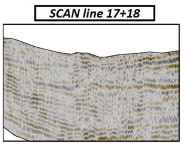
SF5 Shelf-Edge Clinoform Toesets	Diessen Fm.	• Variable amplitude and frequency • Continuous reflectors that pinch out and become highly reflective in one direction, and become wider and fade in the other • Drape the underlying topography (MMU) in the central part of the RVG	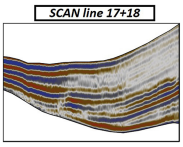
SF6 Shallow water mass transport complex	Diessen Fm.	• Variable amplitude and frequency • Highly reflective top and base • Chaotic reflectors • Occurs nearby faults and below prograding clinoforms	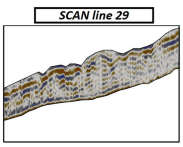
SF7 Current incisions	Diessen Fm. Vrijherenberg Mbr.	• Medium–low amplitude, variable frequency • Higher reflective base and top • Large incisions that vary vertically between 60 and 100 ms TWT and horizontally between 2 and 6 km • Variable shape from U-shaped to V-shaped	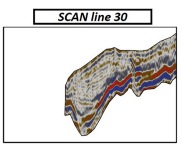
SF8 Shoreface to shallow marine heterolithics	Vrijherenberg Mbr. Veldhoven Fm.	• Variable amplitude, low frequency • Veldhoven Fm. shows slightly lower amplitudes • Continuous, parallel reflectors, conform to underlying and overlying topography • Contains internal low-angle onlap features and incised reflectors	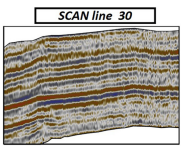
SF9 Coastal swamp/ marshland	Heksenberg Mbr.	• Very high amplitude, high frequency • Continuous but shows breaks due to changing amplitudes or small faults • Facies becomes thicker towards the south-east. Reflectors decrease in amplitude towards the north-west	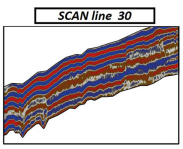

(Continues)

TABLE 2 (Continued)

Seismic facies	Occurrence	Reflection characteristics and geometry	Example seismic cross-section (Height = 0.2 s, width = 6 km) 20× vertical exaggeration
SF10 Shallow Marine Silt and Sand	Kakert Mbr. Vrijherenberg Mbr.	• High amplitude, high frequency • Continuous reflectors • Low-angle truncation of underlying reflectors sometimes, low-angle onlap of overlying reflectors	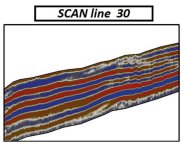
SF11 Slope-fan mass transport complex	Veldhoven Fm.	• Variable amplitude and frequency • Highly reflective top and base • Chaotic reflectors • Occurs nearby faults and contains small faults within	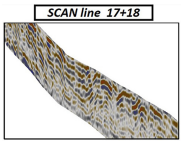

Note: The seismic sections from which seismic facies are derived are indicated above the figures in the right column and can be accessed through the NLOG data portal.

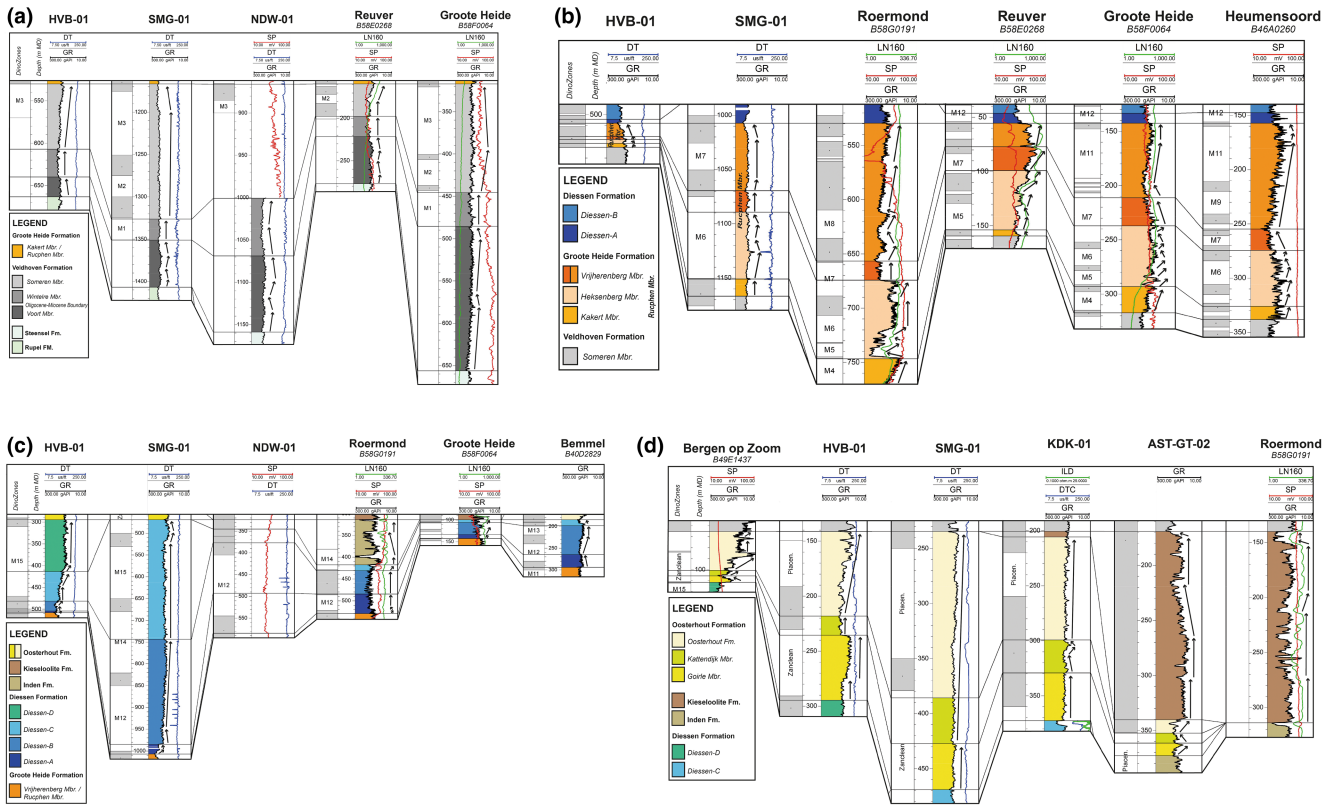

FIGURE 4 Well log correlation panels for (a) the Veldhoven Formation, (b) the Groote Heide Formation, (c) the Diessen Formation and (d) the Oosterhout Formation and Kieseloolite Formation. DT/DTC, sonic log; GR, gamma-ray log; ILD/LN160, resistivity log; SP, Spontaneous potential log. See Figure 3 for locations of the wells and well panel sections.

Correlations show that the Voort Member is present throughout the RVRS and has the greatest in thickness in the eastern part, ranging between 123 and 188 m. The top of the late Oligocene Voort Member is marked on the Campine Block by an erosional unconformity related to the Savian phase, representing a hiatus spanning the late Chattian (late Oligocene) to early Burdigalian (early Miocene) (Vandenberghe et al., 1998) (Figure 2). Consequently, the upper part of the Voort Member, the Wintelre Member and Someren Member are largely missing on the Campine Block. Palynology results from wells along the southern margin of the RVG show the development of this hiatus towards the Campine Block. In well Goirle (Figure 3), for example, a hiatus

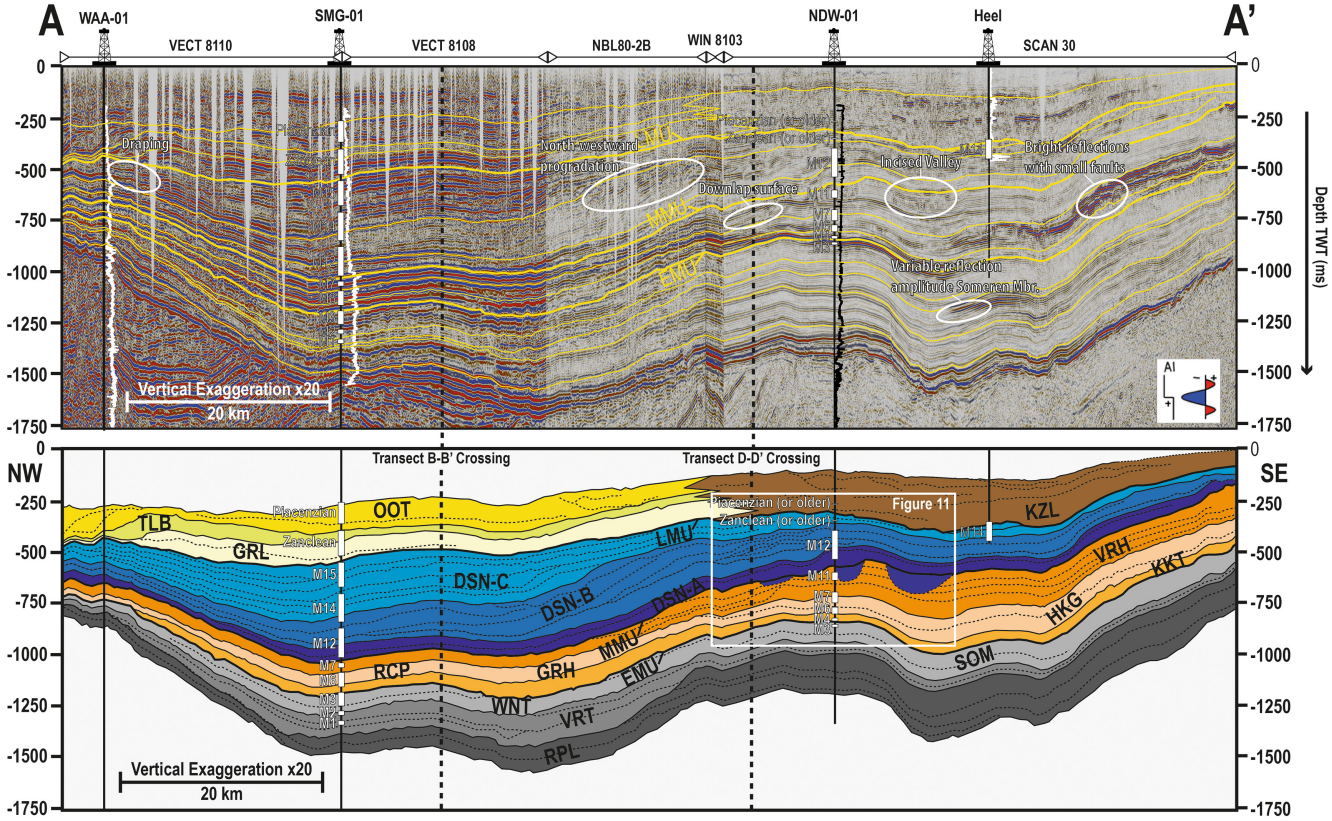

FIGURE 5 NW-SE composite seismic section oriented parallel to the basin axis of the Roer Valley Graben, running through the middle of the Roer Valley Graben. Location of seismic section on Figure 3b. DSN-A/B/C, Diessen Formation A/B/C; GRH, Groote Heide Formation; GRL, Goirle Member (Oosterhout Formation); HKG, Heksenberg Member (Groote Heide Formation); KKT, Kakert Member (Groote Heide Formation); KZL, Kiezeloolite Formation; OOT, Oosterhout Formation; RCP, Rucphen Member; RPL, Rupel Formation; SOM, Someren Member (Veldhoven Formation); TLB, Tilburg Member (Oosterhout Formation); VRH, Vrijherenberg Member (Groote Heide Formation); VRT, Voort Member (Veldhoven Formation); WNT, Wintelre Member (Veldhoven Formation).

encompassing the latest Chattian–earliest Aquitanian is determined. In well HVB-01, early Aquitanian sediments in the overlying Wintelre Member reveal significant reworking from the Eocene–Oligocene and Late Jurassic–Early Cretaceous (Figure 4a). In the more northern part of the RVG, in well SMG-01, no major hiatus was found at the Oligocene–Miocene boundary, but samples from the lowest part of the Wintelre Member have revealed reworking from the Chattian, Rupelian and Eocene. In the central and southern part of the RVG, no major hiatus was observed between the three members of the Veldhoven Formation (Munsterman & Deckers, 2022). In well Reuver (Figure 3), located on the Peel Block, the Oligocene–Miocene boundary is marked by a significant representation of *Homotryblium floripes/plectilum* (45% of the total sum of dinoflagellate cysts). The depositional environment is consequently linked to a restricted marine setting. Thus, observations suggest that the Savian phase resulted in an erosional hiatus in the RVRS on the Campine Block and along the southern margin of the RVG, but not in the RVG, Peel Block and Venlo Block. Overall, the Oligocene–Miocene boundary is characterized by a shallowing of the environment and associated reworking of sediment.

4.1.1.2 | *Wintelre Member*

The Wintelre Member is generally composed of grey to green–grey clays that become siltier and sandier towards the top. An inner-neritic marine depositional environment is interpreted (TNO-GDN, 2024). The unit is present in the Roer Valley Graben, Peel Block and Venlo Block, and varies between 0 and 70 m in thickness. The member is thickest in the central part of the RVG (well AST-GT-02, Figure 3) but is very thin on the Peel Block and Venlo Block, where it loses its distinctive clayey nature towards the northwest. Well logs reveal that the Wintelre Member exhibits slightly higher gamma-ray values compared to the Voort and Someren members. Its base is picked at a peak on the gamma-ray log (Figure 4a). Overall, the Wintelre Member follows a pattern of aggradation, where several small-scale fining-upward successions can be observed in all wells. Especially in well Groote Heide, we observe a pattern of a coarsening-upward succession, followed by several fining-upward successions towards the top, as inferred from the

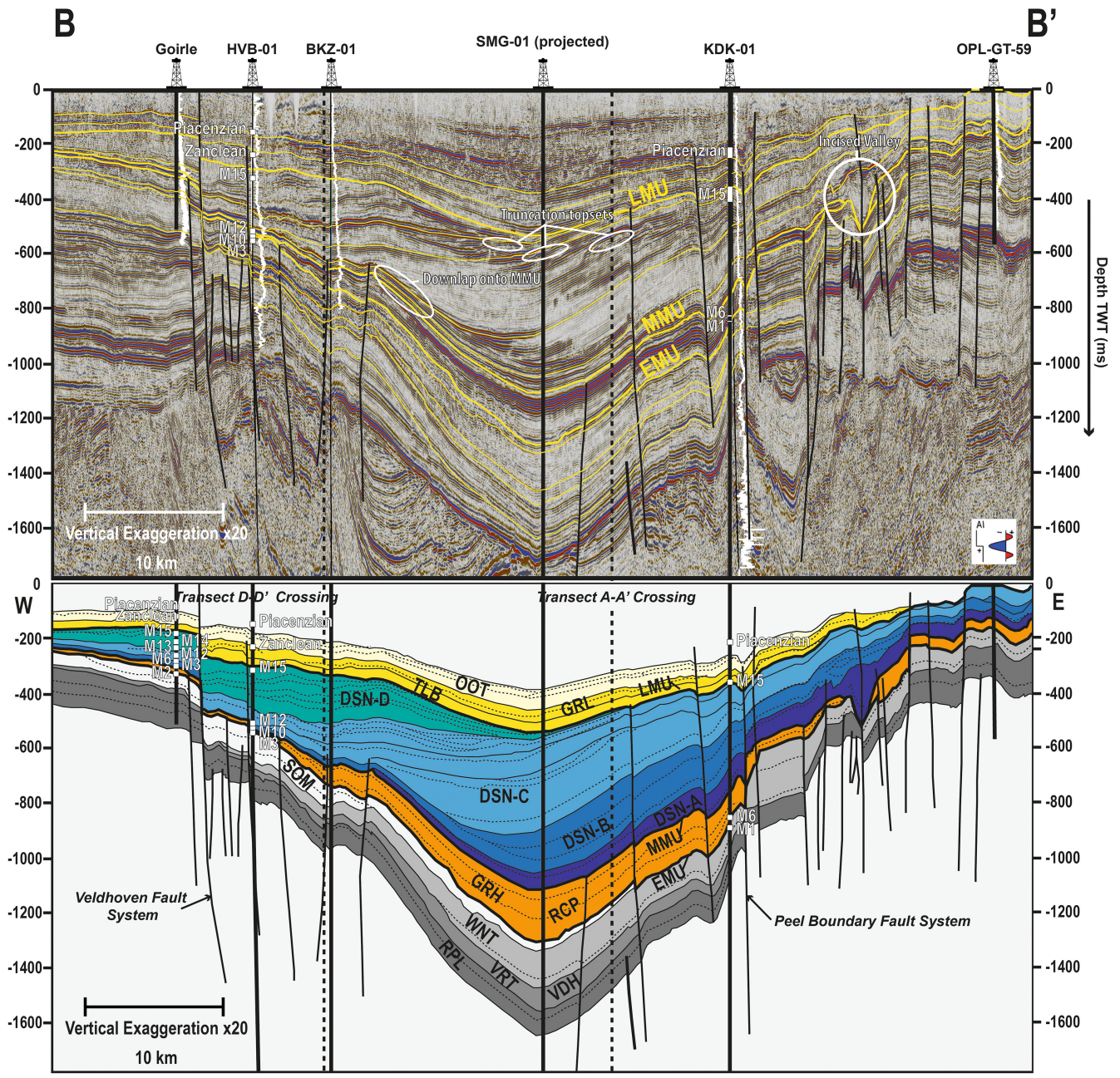

FIGURE 6 WSW-ENE seismic section oriented perpendicular to the basin axis, crossing the northern Campine Block, the central part of the Roer Valley Graben and the Peel Block. Location of seismic section on Figure 3b. DSN-A/B/C/D, Diessen Formation A/B/C/D; GRH, Groote Heide Formation; GRL, Goirle Member (Oosterhout Formation); KZL, Kiezeloolite Formation; OOT, Oosterhout Formation; RCP, Rucphen Member; RPL, Rupel Formation; SOM, Someren Member (Veldhoven Formation); TLB, Tilburg Member (Oosterhout Formation); VRT, Voort Member (Veldhoven Formation); WNT, Wintelre Member (Veldhoven Formation).

gamma-ray and SP logs. The top of the member is picked at a shift towards lower gamma-ray values (Figure 4a). Palynology results link the Wintelre Member to Biozone M1 (*this study*, Munsterman & Deckers, 2020), where high values of the genus *Homotryblium loripes/plectilum* (38%–63%) are revealed in wells Reuver, Groote Heide and Broekhuizenvorst. Additionally, common values of *Paralecaniella* are observed in Broekhuizenvorst. These assemblages are indicative of restricted marine conditions on the Peel Block and Venlo Block. Signs for reworking in the Wintelre Member were found in the RVG in wells SMG-01 and HVB-01.

4.1.1.3 | *Someren Member*

The Someren Member is composed of clayey green–grey sands with low glauconite content that transition upwards into very fine-grained sands. An inner-neritic marine depositional environment is interpreted (TNO-GDN, 2024). The Someren Member is only present in the RVG and south-eastern RVRS, but its age equivalent is also present

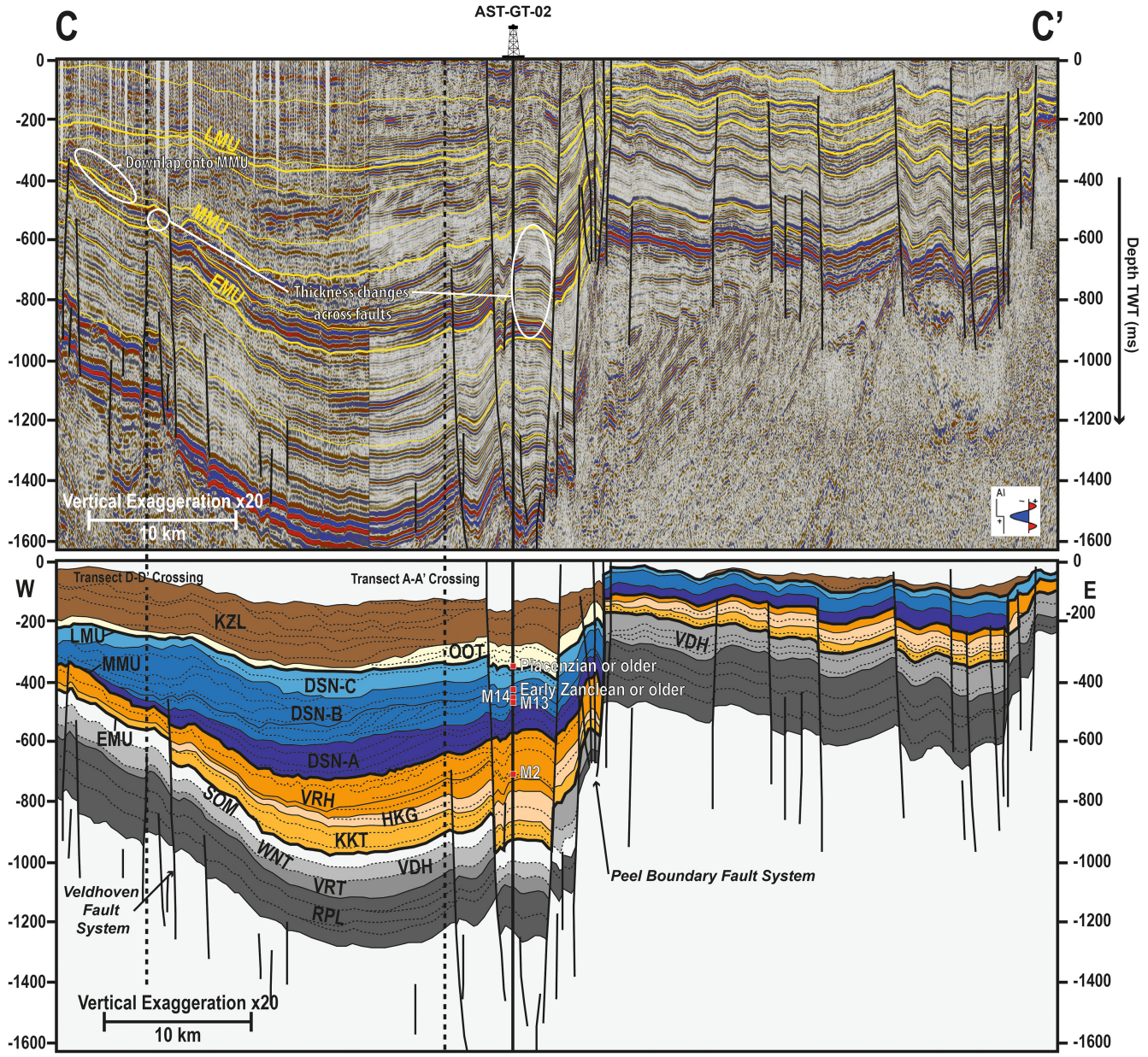

FIGURE 7 WSW-ENE seismic section oriented perpendicular to the basin axis, crossing the south-eastern part of the Roer Valley Graben, the Peel Block and the Venlo Block. Location of seismic section on Figure 3b. DSN-A/B/C, Diessen Formation A/B/C; HKG, Heksenberg Member (Groote Heide Formation); KKT, Kakert Member (Groote Heide Formation); KZL, Kiezeloolite Formation; OOT, Oosterhout Formation; RPL, Rupel Formation; SOM, Someren Member (Veldhoven Formation); VRH, Vrijherenberg Member (Groote Heide Formation); VRT, Voort Member (Veldhoven Formation); WNT, Wintelre Member (Veldhoven Formation).

towards the north-west on the Peel Block and Venlo Block. On the Campine Block, the Wintelre Member is absent and the Someren Member overlies the lithologically similar Voort Member. The member ranges in thickness between 0 and 153 m and shows its greatest thickness in the central part of the RVG, around wells NDW-01 (138 m) and AST-GT-02 (153 m) (Figure 3). Due to its variable thickness and well log characteristics, as well as the difficult distinction between the Voort and Someren members, it may be difficult to identify the lateral and vertical distribution of the Someren Member. In general, the unit is recognized on well logs by an aggrading gamma-ray pattern and shows a coarsening-upward trend in its upper part in wells HVB-01 and Reuver (Figure 4a). The base of the Someren Member is characterized by a shift towards lower-gamma-ray values, when compared to the underlying Wintelre Member. The resistivity logs of wells Reuver and Groote Heide both show an increase towards the top of the Someren Member, which is stronger defined in well Reuver. Combined with an upwards decreasing gamma-ray signal, this points to an overall coarsening-upward succession within the Someren Member.

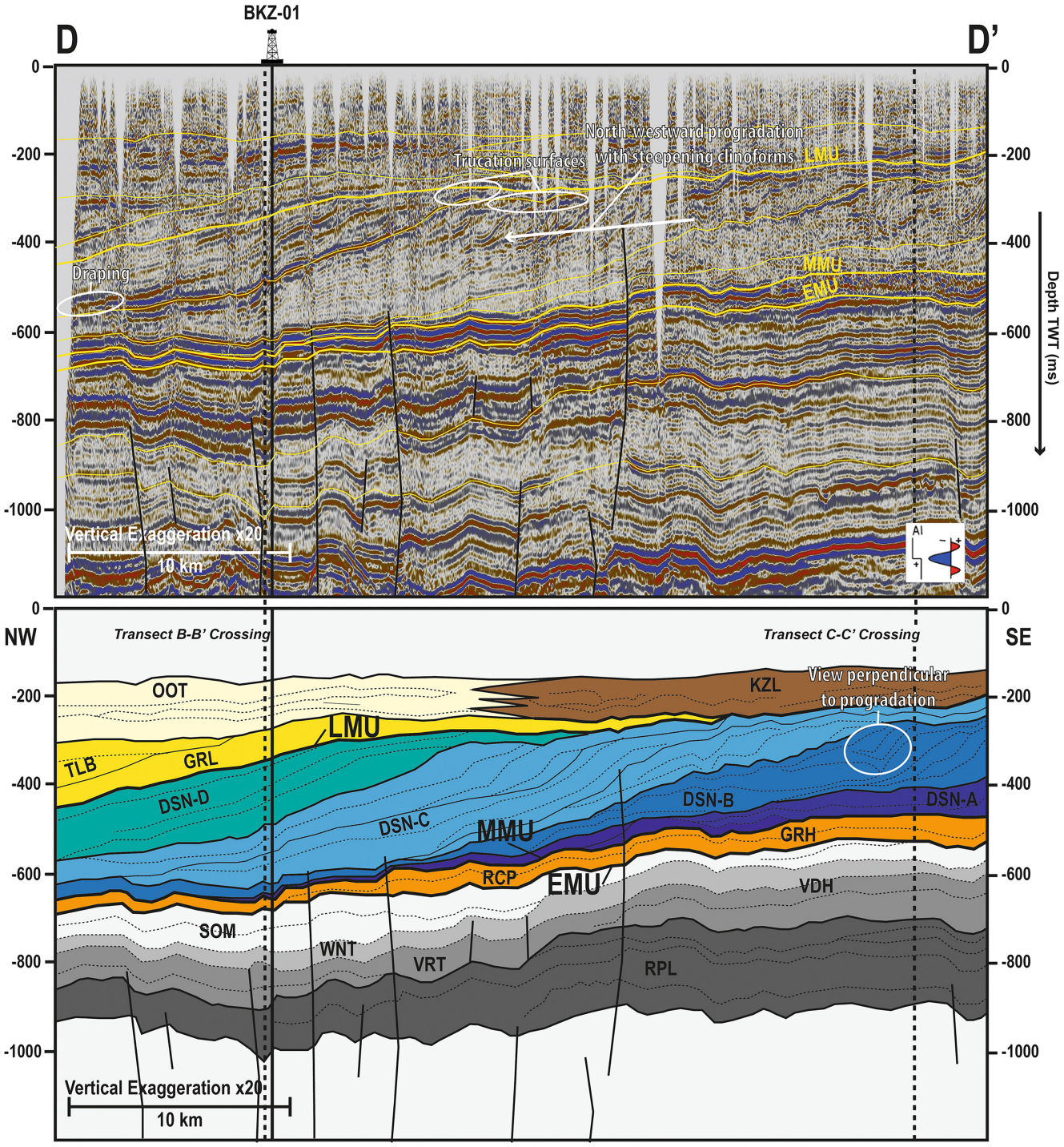

FIGURE 8 NW–SE seismic section oriented parallel to the basin axis, running along the south-westerly margin of the Roer Valley Graben. Location of seismic section on Figure 3b. DSN-A/B/C/D, Diessen Formation A/B/C/D; GRH, Groote Heide Formation; GRL, Goirle Member (Oosterhout Formation); KZL, Kiezeloolite Formation; OOT, Oosterhout Formation; RCP, Rucphen Member; RPL, Rupel Formation; SOM, Someren Member (Veldhoven Formation); TLB, Tilburg Member (Oosterhout Formation); VRT, Voort Member (Veldhoven Formation); WNT, Wintelre Member (Veldhoven Formation).

Dinocyst palynology assigns a late Aquitanian–early Burdigalian age for the Someren Member, corresponding to Biozones M2 and M3. The top is placed between Biozones M3 and M4 and is picked on the gamma-ray log at a peak, indicating a clay- or glauconite-rich layer, followed by a rapid decrease in the gamma-ray signal just above the top of the Someren Member (Figure 4a). In well AST-GT-02 (Figure 3), located in the central RVG, a reworked interval of mainly Chattian (Oligocene) origin was observed in the Someren Member between 710 and 720 m. In a lower

part of the Someren Member (749–860 m), a complete late Palaeocene (Thanetian) association is indicated, with species such as *Alisocysta margarita*, *Areoligera gippingensis*, *Cerodinium depressum* and *Cerodinium* spp. Interestingly, older reworked material is present in the lower part of the Someren Member, while younger reworked material is found in the upper part. This reversal in order suggests differential erosion in the area. More signs of an erosional phase related to either the Savian phase or the EMU were found in the northern part of the RVG, in well HSW-01 (Figure 3). Here, reworking from the Cretaceous and Eocene–Oligocene is present in Biozones M2 and M3. In well Goirle (Figure 3) along the southern margin of the RVG, reworking from the Eocene, Oligocene, Late Jurassic–Early Cretaceous and Carboniferous was identified in Biozone M3. Nevertheless, the dinoflagellate cyst count indicates a marine environment in all three beforementioned wells. Overall, the Someren Member is defined in several wells by lots of reworking, which may also be the explanation to its variable thickness and well log characteristics.

4.1.2 | Groote Heide Formation

From the middle Burdigalian onwards, the Groote Heide Formation and its lateral Belgian equivalent (the Bolderberg and Berchem formations) and German equivalent (the Ville Formation) are deposited in the RVRS. In the southern RVRS, the Groote Heide Formation is divided from bottom to top into the Kakert, Heksenberg and Vrijherenberg members. In the northern RVRS, these members are not distinguishable anymore and are lumped into the Rucphen Member (Figure 2). The Groote Heide Formation is present throughout the RVRS but becomes thin (<50 m) across the Veldhoven Fault System along the southern margin of the RVG (Figure 9). The unit remains thin on the north-western Campine Block. On the south-eastern Campine Block, the formation is thicker, developed around 80 m (Louwye et al., 2020). Well interpretations indicate that preservation of the Groote Heide Formation is variable on the Peel Block. In well Mill (www.dinoloket.nl), for example, the upper part of the Groote Heide Formation, upwards from Biozone M6 is missing, while the succession in well Reuver (Figure 4b) seems to be complete. On the Venlo Block, dinocyst palynology and well log interpretations indicate a continuous record with no significant signs of reworking.

4.1.2.1 | *Kakert Member*

The Kakert Member is composed of yellow–green or greyish to yellow brown very fine to fine sand that can be (moderately to very) silty and glauconitic. The member is marked at its base by a conglomeratic layer with shark

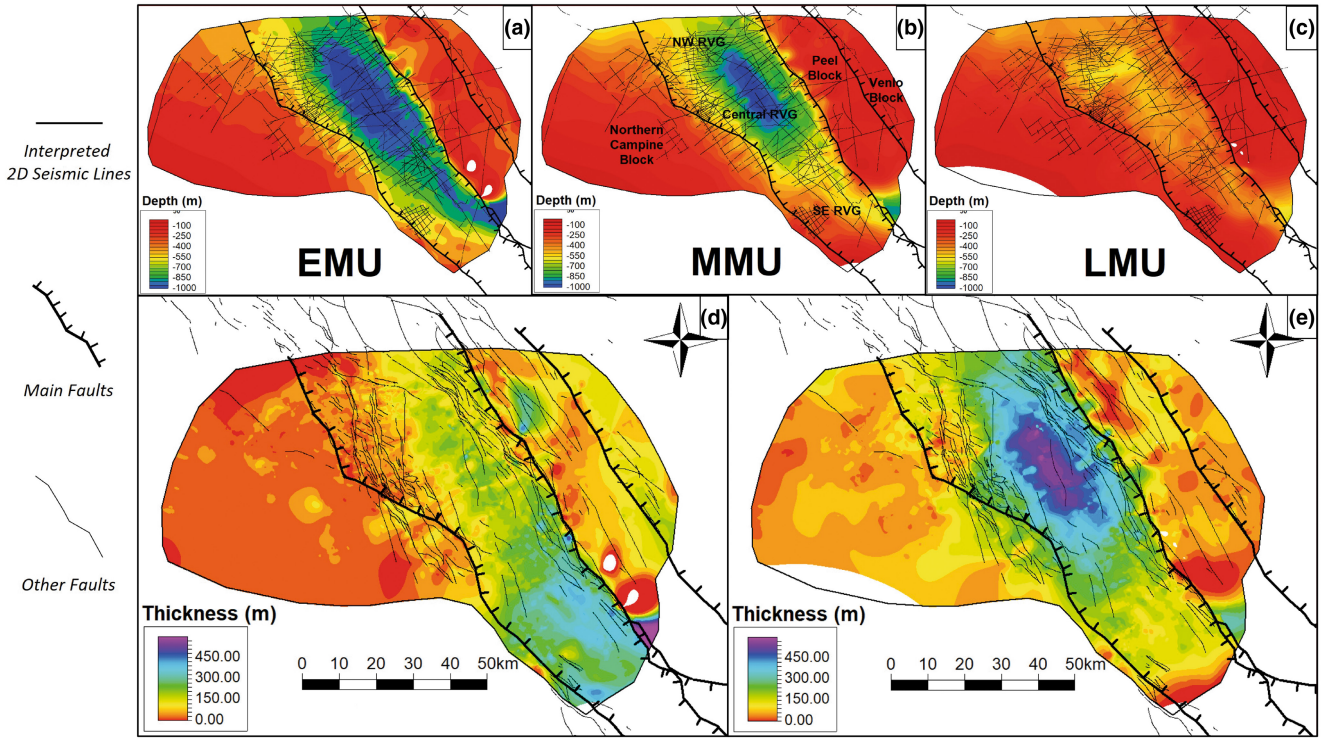

FIGURE 9 (a–c) Depth of the early, mid and late Miocene unconformity in metres. The thin black lines represent interpreted 2D seismic lines for each horizon. (d–e) Thickness maps of the (d) Groote Heide Formation and (e) Diessen Formation, showing the locations of the main depocentres. Time–depth conversion was done using the Velmod-3.1 velocity model (TNO report Velmod-3.1, 2017).

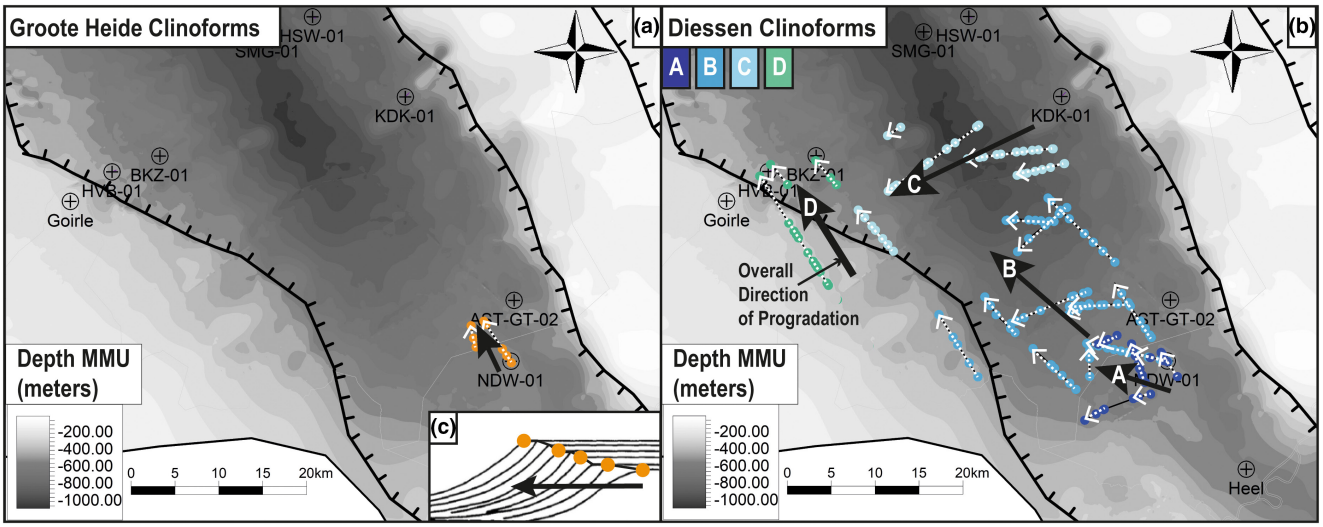

FIGURE 10 Clinoform trajectories mapped on 2D seismic sections. (a) Clinoform trajectories in the Groote Heide Formation and (b) clinoform trajectories in the Diessen Formation. (c) Point sets are based on the position of the rollover point between topset and foreset. Colours of the rollover points indicate different phases of progradation and correspond to the four interpreted subunits of the Diessen Formation. Location of seismic sections in Figure 3b.

teeth, known as the Elsloo Bed. The depositional environment is interpreted as warm shallow marine (TNO-GDN, 2024). In most of the RVRS, the Kakert Member conformably overlies the Veldhoven Formation. On the Campine Block, the Kakert Member unconformably overlies either the Voort Member of the Veldhoven Formation or the lower Oligocene Rupel Formation (Louwye et al., 2020) (Figure 2). The Kakert Member is characterized by intermediate-gamma-ray values between the subjacent Veldhoven Formation and superjacent Heksenberg Member. The base of the unit consequently coincides with a trough on the gamma-ray log, followed by variable patterns recognized throughout the RVRS (Figure 4b). In wells HVB-01 and SMG-01, the Kakert Member is not distinguished anymore, and the associated Rucphen Member encompasses the Groote Heide Formation. In the Rucphen Member, an overall fining-upwards succession is observed. This is contrary to the Kakert Member that is present in the south-eastern RVG, which shows a coarsening-upwards succession that is clearly recognized in well Roermond, for example (Figure 4b). A similar pattern to the Roermond borehole is found in well Groote Heide on the Peel Block. The resistivity log clearly shows an upward increasing trend for wells Roermond, Reuver and Groote Heide, which is again indicative for a coarsening-upward trend throughout the unit. The thickness of the Kakert Member varies between 0 and 34 m in the RVRS, based on well correlations, and is thickest in the central part of the RVG (e.g. well AST-GT-02, Figure 3). It thins towards the north and north-west, where the unit transitions into the Rucphen Member. The Kakert Member corresponds to Biozones M4-6 (late Burdigalian–early Langhian) (Munsterman & Deckers, 2022). In the northern part of the RVG, well HSW-01 (Figure 3) shows limited reworking of dinocysts from the Carboniferous, Jurassic–Cretaceous and Eocene–Oligocene in Biozone M4 (Rucphen Member). Palynology results from the same time interval in wells Groote Heide and Broekhuizenvorst on the Venlo Block report a dominance of terrestrial spores and pollen, while the variety of marine dinoflagellate cysts decreases. Notably, the species *Pediastrum* was abundantly found in well Groote Heide around the transition between Biozones M4 and M5. This type of algae has a fresh-to-brackish water distribution, referring to an influx of freshwater and circumstances of reduced salinity. The increase in terrestrial spores and pollen towards the top of the Kakert Member is a further indication of shallowing towards a marginal marine or coastal setting (Louwye et al., 2020). The highest peak in *Pediastrum* is found in the lower part of the Heksenberg Formation, in Biozone M5 (282–284 m and 288–291 m), where the species represents 41% of the total palynomorph assemblage. The shallow marinel influence in the Kakert Member is also reported in the Belgian time equivalent Houthalen Member, in which a shallowing towards the top is indicated by the local presence of lignite during the late Burdigalian (Deckers & Louwye, 2019). Overall, the log characteristics and palynological results match well, testifying a progressive shallowing environment during deposition of the Kakert Member.

4.1.2.2 | *Heksenberg Member*

The Heksenberg Member consists of white-to-grey, fine-to-medium sand, intercalated with lignite seams. The latter occur in two stacked clusters. The top and base of the Heksenberg Member are commonly marked by a layer of

rolled flint. The depositional environment is interpreted as coastal lowland, including a beach and intertidal setting (TNO-GDN, 2024). As the Heksenberg Member contains less glauconite than the Kakert Member, the base of the Heksenberg Member can be identified on well logs by an upwards decrease in gamma-ray values (Figure 4b). The upper boundary of the Heksenberg Member is marked by an increase in gamma-ray values towards the glauconite-bearing silty sands of the Vrijherenberg Member. Within the member, we observe several coarsening-upward successions, which can be well observed in wells Roermond, Reuver and Groote Heide in the south-eastern RVRS (Figure 4b). Here, the Heksenberg Member can be clearly recognized by overall low-gamma-ray values, interrupted by sharp peaks and troughs. These spikes in the gamma-ray log correspond with clay-rich layers and the gamma-ray troughs with lignite layers. From well NDW-01 towards the north-west, the distinctive coarsening- or fining-upwards successions of the Heksenberg Member disappear (Figure 2). This transition to more homogenous deposits in the Groote Heide Formation characterizes the transition to the Rucphen Member, where the typical Heksenberg Member's facies of marginal marine sand with lignite is absent, but its age-equivalent open-marine facies is present.

Dinocyst assemblages assign an age to the Heksenberg Member ranging from the latest Burdigalian to the Langhian, corresponding to the M4-6 and early M7 Biozones (Munsterman et al., 2019). In well Roermond, in the southern part of the RVG (Figure 4b), the succession shows a facies that is poor in marine dinoflagellate cysts but rich in bisaccate pollen. Furthermore, *Botryococcus*, a fresh-to-brackish water algae is well represented throughout this interval, indicative of a near-coastal, marginal marine, to estuarine environment. Most striking is the interval at 739.2–743.4 m depth, where a 'mega' reworking is reported on top of a rapidly fining-upward succession, including numerous Mesozoic sporomorphs and high numbers of species known from the Posidonia Shale Formation of Toarcien age (Early Jurassic). This reworked interval corresponds to Biozones M4-6 in the lowest part of the Heksenberg Formation. On well logs, this interval is located just above an interval with strongly increasing gamma-ray values between 744 and 746 m depth (Figure 4b). The resistivity log shows less severe changes, but indicates gradually decreasing values, pointing to an overall fining-upwards succession. This facies is described as very near-coastal, marginal marine to estuarine. The heavy reworking is very likely influenced by the nearby position of the Peel Boundary Fault System. Across this fault system, on the Venlo Block, the Groote Heide borehole was sampled in high resolution for dinocyst species analysis. Three transgression–regression cycles are described within the Heksenberg Member, starting with a transgression at the base. The analyses show a drop in restricted marine species and growth of open marine taxa between Biozones M4 and M5, around the boundary between the Kakert Member and Heksenberg Member. This transgression is immediately followed by a regression, as inferred from the total palynomorph assemblage including 41% *Pediastrum* between 288.6 and 291.6 m. Their concentration remains high up to 282.1 m, covering a large part of Biozone M5. A growing number of *Paralecaniella* and a peak in bisaccates is observed between 271.8 and 273.8 m, corresponding to the transition between Biozones M5 and M6. A transgression manifests again later on in the Langhian between 265.8 and 273.8 m depth, in the lower part of Biozone M6, where *Pediastrum* and *Paralecaniella* are present in low numbers. Biozone M7 between 239.8 and 240.1 m is characterized by low numbers of restricted and shallow marine dinoflagellate cysts and peaking open marine species. Their ratios gradually change in the favour of restricted marine species up to 226.8 m depth, marking the uppermost part of the Heksenberg Member.

In the north-western RVRS, the glauconite-rich sands of the Rucphen Member hold similar Biozones as the Heksenberg Member, which indicates a facies transition from south-east to north-west. At the top and base of Biozone M6 in well NDW-01 (Figure 11), an increased number of palynomorphs typical of shallow water and/or restricted systems (e.g. *Polysphaeridum zoharyi* and *Paralecaniella* spp.) is observed. Indications for this depositional environment are consistent with the Heksenberg Member in boreholes located further south-east. Some lignite layers are also mentioned in at the stratigraphic level of the Heksenberg Member in well NDW-01, around 800 m depth. However, a scarcity of terrestrial sporomorphs in well NDW-01 between 785 and 825 m depth indicates a relatively distal setting still during the middle Langhian. It is therefore our interpretation that at the location of well NDW-01, the Heksenberg Member transitions into the Rucphen Member as the bathymetry increases towards the north-west, and the continental influence gradually decreases. In wells SMG-01 and KDK-01, Biozone M6 is present and is dominated by marine dinocysts.

4.1.2.3 | *Vrijherenberg Member*

The Vrijherenberg Member consists of brownish yellow-to-greenish fine sand with silt and is commonly glauconitic. Its depositional environment is interpreted as shallow marine to coastal (TNO-GDN, 2024). The Vrijherenberg Member is the youngest unit within the Groote Heide Formation and has a thickness range of 0–155 m. Its palynological record is complete in the RVG and Venlo Block and the member is thickest developed in the central and southern RVG, as observed in wells

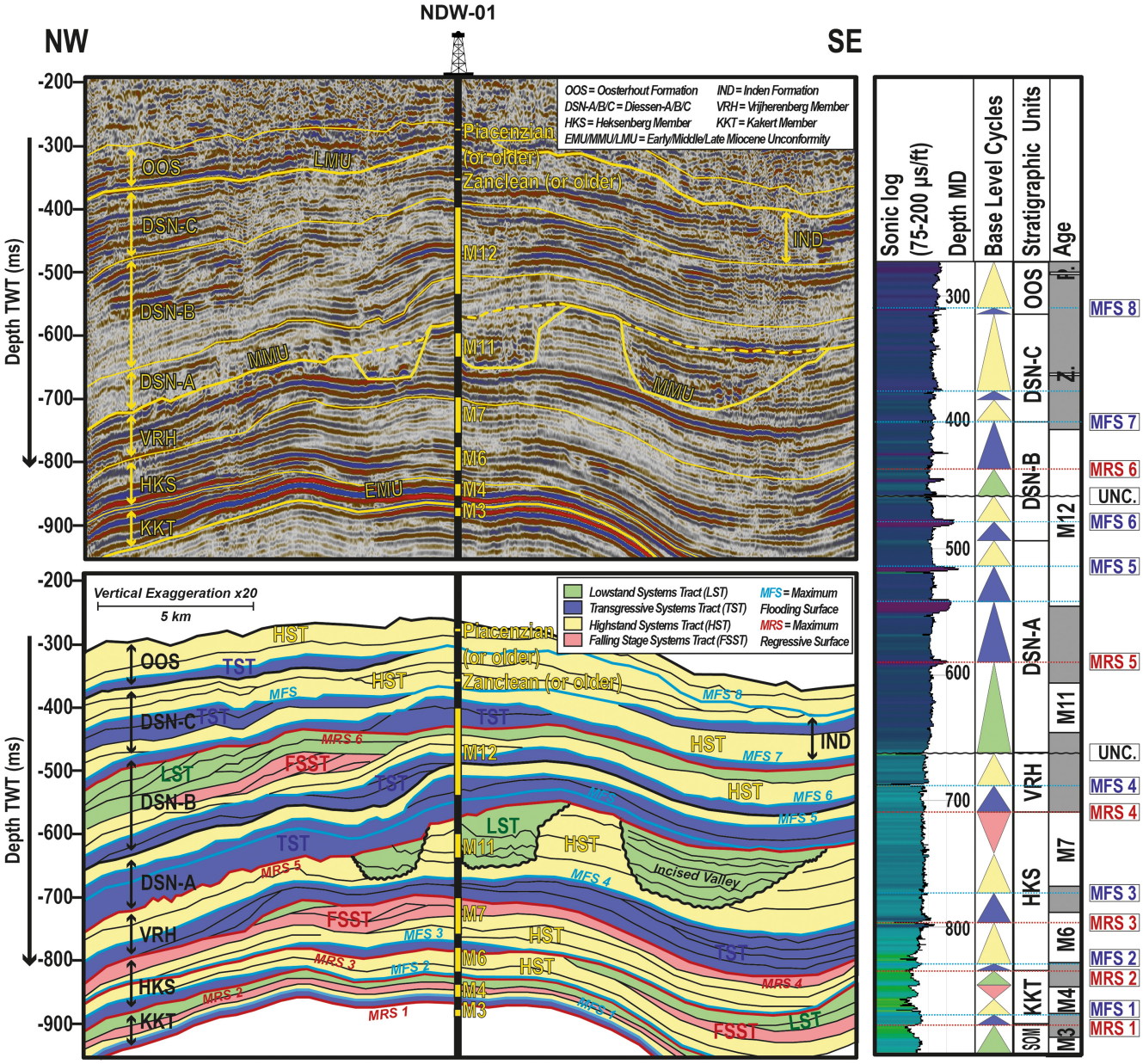

FIGURE 11 Sequence stratigraphic relationships of the Groote Heide and Diessen formations. UNC, Unconformity. Interpretations are based on a part of section A–A′ (Figure 5). Sequence stratigraphic relationships are based on principles as described by Catuneanu (2006), Catuneanu et al. (2011) and Helland-Hansen and Hampson (2009). On the right, well NDW-01 is displayed, including the sonic log, age, stratigraphic position and interpreted base-level cycles.

MLB-L4, NDW-01 and Roermond (Figure 3). The member is truncated at the top on the Peel Block, as inferred from (partially) missing dinocyst records. Towards the south, on the Campine Block, the Vrijherenberg Member (Belgian Molenbeersel Formation) is absent and the Heksenberg Member (Belgian Genk Member) is directly overlain by the Diessen Formation (Belgian Diest Formation) (Deckers & Louwye, 2019). The lower boundary of the Vrijherenberg Member is characterized on the gamma-ray log by a distinct shift to higher values, corresponding to an increased glauconite content (e.g. wells Roermond, Reuver and Heumensoord; Figure 4b). In wells Heumensoord and Groote Heide, a fining-upward succession in the lower part of the Vrijherenberg Member can be observed, followed by a coarsening-upwards succession in the upper part of the Vrijherenberg Member. Well SMG-01 shows the same trends in the Rucphen Member. In well Roermond, several coarsening-upwards successions are even observed in the upper part of the Vrijherenberg Member. In well Reuver, the lower part of the member misses the characteristic fining-upward succession. Nevertheless, a distinct peak on the gamma-ray log is observed around 77 m depth, marking the same maximum flooding surface (MFS) around Biozones M7

and M8 (Figure 4b). The SP and resistivity logs indicate an overall coarsening-upward succession throughout the member in well Groote Heide. In well Roermond, the introduction of *Botryococcus* and *Paralecaniella* marks the transition from shallow-open marine conditions in Biozone M8 to marginal marine to estuarine conditions in Biozones M9 and M10, indicative of progressive shallowing. In well Reuver located on the Peel Block, Biozones M9-11 are even missing, highlighting a hiatus in the top of the Vrijherenberg Member. A different trend was observed in well Groote Heide. A transgressive phase was recorded in the lower part of the Vrijherenberg Member between 217.8 and 220.8 m, evidenced by the diminishing number of restricted marine species. A highstand follows between 211.4 and 196.3 m, with a maximum appearance of open marine dinoflagellate cysts between 196.3 and 199.3 m, and a minimum of restricted and shallow marine species between 193.9 and 196.3 m. This occurs in Biozone M9 and M10, which also shows maximum-gamma-ray values, thus representing a maximum flooding surface (MFS). The MFS is followed by a highstand phase recorded between 193.55 and 159.8 m in well Groote Heide, encompassing Biozone M11. *Paralecaniella* dominates most of the succession here (42%–69%). Lower-gamma-ray values and high number of *Paralecaniella* in the top of the Vrijherenberg Member are also observed in wells Heumensoord and Broekhuizenvorst on the Venlo Block, indicating maximum regression. Also, in well NDW-01, in the central part of the RVG, Biozone M11 is characterized by upwards diminishing numbers and dinoflagellate species, except for *Spiniferites* spp. This may be associated with regression and shoaling (Hultberg & Malmgren, 1986). In well Roermond, in the south-eastern RVG, a maximum regressive surface (MRS) was identified from dinocyst palynology around 530 m depth between Biozones M11 and M12. The recorded events in wells Roermond, Reuver, Groote Heide and NDW-01 mark a transgressive phase during the late Serravalian (Biozones M8-10), followed by a highstand and possibly regressive phase during the earliest Tortonian (Biozone M11) during which the environment shallows. A final regressive and lowstand during the early Tortonian marks an erosional phase on the Peel Block. The latter is associated with the formation of the mid-Miocene unconformity (MMU) encompassing Biozones M11 and M12. This phase is also linked to the formation of the incised valleys of Figures 5 and 11. The transition towards the superjacent Diessen Formation corresponds to an upwards increase in glauconite content, expressed by an overlying increase in gamma-ray values that is visible in most wells in the RVRS. In well Reuver, this increase in gamma-ray values is very abrupt, while in other boreholes, it is more gradual.

4.1.2.4 | *Rucphen Member*

The Rucphen Member is composed of dark green to black, very glauconitic, fine-to-very coarse sand that can be slightly silty or clayey. Its depositional environment is interpreted as shallow marine (TNO-GDN, 2024). As it is richer in glauconite compared to the subjacent Veldhoven Formation and superjacent Diest Formation, the lower and upper boundaries coincide with respectively upwards increasing and upwards decreasing in gamma-ray values (Figure 4b). The Rucphen Member generally attains very-high-gamma-ray values. Thicknesses are over 100 m in boreholes HSW-01 and SMG-01 in the northern RVG (Figures 3 and 4b) and strongly decrease across the western border fault system of the RVG towards values of less than 30 m on the Campine Block. In wells SMG-01 and HSW-01, the unit holds the M4 to M11 Biozones, where palynological assemblages indicate an open marine environment.

4.1.3 | Diessen Formation

The late Miocene (Tortonian–Messinian) Diessen Formation and its lateral Belgian equivalent (Diest Formation) and German equivalent (Inden and Kieseloolite Formation) are present throughout the RVRS (Figure 2). The formation is thickest in the northern part of the RVG, and strongly thins towards the south-eastern RVRS (Figure 9). The location of major thickening takes place between wells Roermond and NDW-01 (Figure 4c). In well Roermond, the early Tortonian M12 Biozone is at least 57 m thick, and in well NDW-01, its thickness has increased to at least 140 m. Further north-west, in well SMG-01, the late Tortonian M13 and M14 Biozones in the Diessen Formation are also each over 100 m thick. The latest Tortonian–Messinian M15 Biozone is thickest developed in the northern RVG, such as around wells HVB-01 and SMG-01. The latter Biozone is not observed in the southern RVG, however, where a transition from the marine Diessen Formation to the fluvial Kieseloolite Formation takes place during the late Miocene and dinoflagellate cyst percentages diminish. The majority of the M14 Biozone here is held by the transitional Inden Formation (Figure 4c). In the north-western RVRS, the Diessen Formation overlies the Rucphen Member of the Groote Heide Formation. Since the latter is richer in glauconite than the Diessen Formation, the base of the Diessen Formation corresponds to a decrease in gamma-ray values. In well Roermond, the Diessen Formation overlies the Vrijherenberg Member. Since the top of the Vrijherenberg Member is relatively poor in glauconite (end of a regressional phase), the base of the Diessen Formation here corresponds to an upwards increase in

gamma-ray values. In wells Goirle, HVB-01 and SMG-01, the basal section of the Diessen Formation still has relatively high-gamma-ray values (Figure 4c). This might be due to reworking of glauconite from the subjacent Rucphen Member. In general, gamma-ray logs indicate overall lower values in the Diessen Formation compared to the Groote Heide Formation, suggesting less clay-rich and/or less glauconite-rich sediment. Most wells also show several coarsening-upward successions towards the top of the Diessen Formation (e.g. wells Bemmel and HVB-01). Based on well logs and palynological data, the Diessen Formation can be subdivided into four units, Diessen-A, -B, -C and -D. These sub-units can also be discriminated seismically as seismostratigraphic units, as discussed later in this work (Section 4.2, Figures 5–8).

4.1.3.1 | *Diessen-A*

Subunit Diessen-A is characterized by a sharp peak on the gamma-ray log at its base, followed by a rapid decrease. Towards the top of Diessen-A, values increase gradually, indicating a fining-upward succession. This trend is observed in most wells, including all wells in Figure 4c. The SP and sonic logs exhibit a more or less aggrading pattern (e.g. wells Roermond and Groote Heide), where the sonic log tends to be a bit more rugged around the middle of Diessen-A (wells NDW-01 and SMG-01). In well SMG-01, a peak is observed at the top the fining-upward succession, around a possible maximum flooding surface (MFS). Diessen-A is associated with the lower part of Biozone M12, indicating an early Tortonian age. Dinoflagellate cyst palynology from Biozone M12 in well NDW-01 points to a reduced terrestrial debris and an increase in the number and variety of dinoflagellate cysts, in particular *Spiniferites* spp. Some reworking of the middle Miocene is also present here. These findings support a deeper marine condition during deposition of Diessen-A, compared to deposits from the upper part of the Vrijherenberg Member. The same transgressional features are described in well Roermond, where palynological evidence suggests a change from estuarine conditions to shallow marine conditions with estuarine influence from Biozone M11 to M12, as inferred from an increase in marine dinoflagellate cysts and a slight reduction in the numbers of the restricted marine species *Paralecaniella* and *Botryococcus*. In well Groote Heide, a transgression was recorded between 132.8 and 135.8 m in Diessen-A. This is confirmed by a very sharp drop in the percentage of *Paralecaniella* from 65% to 3%. According to the ratio between terrestrial and marine sporomorphs, this transgressive phase already begun from 156.8 m depth. This transgression is followed by a highstand between 128 and 132.8 m, as inferred from an increasingly extensive group of shallow marine taxa in the dinoflagellate cyst assemblage. The highstand phase occurs in Diessen-B.

4.1.3.2 | *Diessen-B*

The boundary between Diessen-A and Diessen-B is marked by a shift in the gamma-ray signal towards lower values. This can be clearly observed in wells Reuver, SMG-01 and HVB-01 (Figure 4c). In wells Groote Heide and Bemmel, the transition is very subtle. The shift towards lower values is followed by an overall coarsening-upwards succession towards the top of Diessen-B in wells Bemmel and HVB-01, for example. Wells SMG-01, NDW-01 and Roermond show a more aggradational pattern towards the top of Diessen-B. The sonic log reveals distinct troughs in travel time within Diessen-B, indicative for hard layers (NDW-01 and SMG-01). Lithological descriptions from well SMG-01 indicate the presence of carbonates around these hard layers. The presence of carbonate may be an indication for low-energy conditions during deposition. Dinocyst palynology links Diessen-B to the upper part of Biozone M12 and to Biozone M13, corresponding to a Tortonian age. In well NDW-01, some reworking from the middle Miocene was found in Biozone M12 (405–545 m). The dinoflagellate cyst assemblage nevertheless shows a high number of *Spiniferites* spp. here, indicative of open marine conditions. Towards the south-east, well Roermond reveals limited reworking from the Upper Jurassic–Lower Cretaceous in Diessen-A and the lower part Diessen-B (464.5–522.2 m). The association indicates a moderate presence of marine dinoflagellate cysts, a dominance of bissacate pollen, and the presence of *Pediastrum*, *Botryococcus* and *Paralecaniella*, pointing to shallow marine conditions with an estuarine influence. The upper part of Diessen-B (446.5–449.5 m) is characterized by an association dominant in sporomorphs and bisaccates pollen, including the presence of *Homotryblium* sp., *Paralecaniella* and *Botryoccus*, suggestive of a near-coastal to marginal marine setting. These consecutive observations reveal a gradual regression towards the top of Diessen-B. In well Reuver on the Peel Block (Figure 3), the top of Diessen-B is marked by a significant increase in Paralecaniella (46% of the total sum of palynomorphs), suggesting a shallowing phase during the transition from Diessen-B to Diessen-C. In north-western direction along the Venlo Block, well Bemmel reveals a relatively high amount of marine reworking (c. 8%) from older stratigraphies at the top of Diessen-B around 200 m, corresponding to Biozone M13. No indications for marginal marine conditions were evidenced here. Overall, palynomorphs assemblages from Diessen-B evidence a general decreasing marine influence towards the top of the unit, with estuarine influence in the central and southern RVG, near-coastal conditions on the Peel Block and Venlo Block and gradually increasing open marine conditions towards the north-west.

4.1.3.3 | *Diessen-C*

The base of Diessen-C is marked by a shift towards lower values in the gamma-ray signal, which can be observed in wells HVB-01, Reuver, Groote Heide and Bemmel (Figure 4c). An aggrading sequence is evident in well SMG-01 that is similar to Diessen-B, but a coarsening–fining-upward succession is clear in the upper part of Diessen-C. Wells Groote Heide and Bemmel on the Venlo Block reveal a coarsening-upward succession, followed by a fining-upward succession, and a spikey aggrading sequence towards the top of the Diessen Formation. The top of Diessen-C is characterized by a peak on the gamma-ray log, followed by a sequence with lower-gamma-ray values. Diessen-C is linked to Biozones M14 and the lower part of M15, corresponding to a late Tortonian-to-Messinian age. Chronologically, Diessen-C is concurrent with the Inden Formation, which emerges from the south-east during the same time. The Inden Formation forms the more proximal, fluvial equivalent of the more distal, marine Diessen-C. In well Heel (seismic Section A–A′, Figure 5), the interval between 385 and 395 metres depth, associated with Biozone M14, indicates the presence of freshwater species within the Inden Formation. A subsequent flooding event at 360 MD indicates a brief marine ingression. The results highlight a multifaceted transition from the marine Diessen Formation to the Inden Formation. Towards the north-west (e.g. wells HVB-01 and HSW-01), the lower part of Diessen-C shows signs of reworking from older sequences. As mentioned in the previous section about Diessen-B, this may be related to a phase of maximum regression around the transition between Diessen-B and Diessen-C. The upper part of Diessen-C is characterized as predominantly marine again. In well Roermond, Diessen-C was interpreted between 420 and 430 m. Palynological analysis from Biozone M14 (425.5–428.5 m) reveals that the component of marine dinoflagellate cysts is 63% of the total sum of palynomorphs here. A fresh-to-brackish water algae (*Botryococcus*) is also present. A shallow marine setting with estuarine influence is plausible. Well Roermond also contains the Inden Formation between 313 and 420 m depth, as interpreted in this study. The palynological association of a sample at 379.5–381.5 m depth shows that the assemblage is dominated by bissacate pollen (80%), while 20% of the palynomorphs is marine. This reveals a gradual transition between the Diessen Formation and the Inden Formation.

4.1.3.4 | *Diessen-D*

Diessen-D represents the youngest subunit within the Diessen Formation and is solely present as a thick wedge along the Veldhoven Fault System (Figures 6 and 8). Boreholes Goirle, HVB-01 and BKZ-01 reveal a consistently upwards, decreasing gamma-ray signal that corresponds to a coarsening-upward trend. Diessen-D also has an overall lower gamma-ray response compared to Diessen-A, -B and -C. The base is marked by a peak in the gamma-ray signal, possibly related to a clay-rich layer associated with marine flooding. Unfortunately, no palynological records regarding the depositional environment of Diessen-D are available. The transition between the Diessen Formation and either the Oosterhout Formation or Kieseloolite Formation is associated with the late Miocene unconformity (LMU), as described in Munsterman et al. (2019). In the north-western RVRS, we observe a sharp decrease in gamma-ray log values at the LMU surface. In borehole HVB-01, for example, the LMU is interpreted at 275 m based on a distinct shift to lower gamma-ray values above it, associated with the transition from the Diessen Formation to the Goirle Member (Oosterhout Formation). From lithological descriptions, this observation reflects a change from glauconite-rich silts and sands of the Diessen Formation to the coarser glauconite-poor sands with abundant shells of the Oosterhout Formation. Alternatively, in the south-western RVRS, the LMU is marked by a transition to a spiky gamma-ray pattern resulting from clay-sand–gravel alterations of the Kieseloolite Formation. Both transitions are indicative of a regionally shallowing environment. Palynological analyses confirm this. In well SMG-01, sporomorphs and freshwater algae dominate the spectrum in the early Pliocene, whereas the marine component increases gradually downwards in the latest Miocene. The same trend is evident in wells KDK-01, AST-GT-02, NDW-01, Roermond and Groote Heide (Figure 3). Reworking in the late Miocene–early Pliocene deposits was also evidenced in wells Groote Heide and HVB-01. Interestingly, despite the absence of Diessen-D along the northern rim of the RVG and in the south-eastern RVRS, no significant time hiatus was evidenced based on palynological dating. Both wells HVB-01 along the southern rim of the RVG, and wells SMG-01, KWK-01 and KDK-01 along the northern rim of the RVG, contain a significant latest Miocene sequence associated with Biozone M15 that highlights a gradual shallowing towards the end of the Miocene. In the south-eastern RVRS, a possible hiatus between the Diessen Formation and Kieseloolite Formation is difficult to identify, since the fluvial Kieseloolite Formation does not contain dinoflagellate cysts anymore to determine the depositional age of the sediment.

4.1.4 | Inden Formation and Kieseloolite Formation

During the latest Miocene, the lithofacies show a strong differentiation between the south-eastern and

north-western RVRS. In the north-western RVRS, deposition of the Diessen Formation continues throughout the Tortonian and Messinian up to the boundary with the Pliocene, where the unit transitions into the Oosterhout Formation. In the south-eastern RVRS, the upper Tortonian is characterized by the deposition of sands from the Inden Formation that diffusely transitions into the fluvial deposits of the Kieseloolite Formation on top of the early-to-middle Tortonian marine deposits of the Diessen Formation.

The Inden Formation is composed of dark grey medium-to-very-coarse sand. Locally it can contain gravel or be clayey with lignite seams and wood fragments. Its depositional environment is interpreted as littoral and coastal lowland, including swamp, floodplain and meander deposits (TNO-GDN, 2024). The unit is only present in the southern RVG and thins in north-western direction. Its gamma-ray log signature is characterized by very low values, interbedded by thin clay beds that reflect sharp spikes on the log (Figure 4d). Dinoflagellate cyst assemblages assign the Inden Formation to Biozone M14. This has been recorded in wells Heel and Roermond in the southern RVG. The palynological assemblage of well Roermond shows a dominance of bisaccates pollen (98%) and absence of marine dinoflagellate cysts in the Inden Formation. In the lower part of the unit, the number of bisaccates pollen is reduced, but still dominant (80%). Nevertheless, 20% of the association is marine. Of the marine component, 35% comprises the species *Operculodinium centrocarpum*, an opportunistic taxon which is more frequently present under changing depositional circumstances. Below the Inden Formation, the marine component rapidly increases to 63%, indicative of the Diessen Formation, which is still present here and falls in Biozone M14 as well. In well Heel, a flooding event was recorded around the middle of the Inden Formation, evidenced by an increase in marine species and the occurrence of a clay-rich layer.

The Oosterhout Formation and Kieseloolite Formation are chronologically more or less equivalent, but the more proximal Kieseloolite Formation starts developing in the south-eastern RVRS during the latest Miocene, whereas the more distal Oosterhout Formation in the north-western RVRS develops from the earliest Pliocene (Figure 2). The formations gradually transition into one another and may interfinger and coexist in certain wells, such as boreholes KDK-01 and AST-GT-02 (Figure 3). The coarse sands of the Kieseloolite Formation extend from the south-east up to well KDK-01 in the north-west. The gamma-ray pattern is characterized by low values, indicative of clean sands. Spikes occur on top of the low-gamma-ray background, which correlate to clay layers, sometimes containing lignite (Figure 4d). In well AST-GT-02, the palynological assemblage shows a limited number of palynomorphs and diversity, notably lacking marine dinoflagellate cysts. Macerals, representing organic matter in coal-forming peat, are relatively abundant compared to palynomorphs. Also, in well KDK-01 at the northern extended margin of the Kieseloolite formation, freshwater species, poor preservation of marine microfossils and a relatively high abundance of sporomorphs are noted in the unit. Palynological dating of the Kieseloolite Formation is not available, due to the paucity of palynomorphs. Chronostratigraphically significant species were not present in the samples of our well selection.

4.2 | Seismic interpretations

The stratigraphic units based on and characterized by well logs and biostratigraphy have been mapped on seismic sections. The reflection characteristics, seismic facies analysis and the stratal patterns of the units (Figures 5–8) are used to further characterize them and constrain their depositional environment (Table 2). Furthermore, depth maps and thickness maps are constructed to infer the spatial distribution of the two major stratigraphic sequences: the Groote Heide Formation and the Diessen Formation (Figure 9).

4.2.1 | Seismic characteristics of the Veldhoven Formation

The Veldhoven Formation is generally characterized on seismic data by low-frequency, low-amplitude reflections that show a large continuity, assigned to seismic facies SF8 (Table 2).

4.2.1.1 | *Voort Member*

The Voort Member is expressed by a series of conformable, low-frequency, variable amplitude reflections. Its base is picked at a hard-kick (blue) reflection, representing the transition from the underlying Rupel Formation to the Veldhoven Formation. No large erosional features are observed on seismic sections, except along the southern rim of the RVG, where small incisions and low-angle truncational features are observed around the base of the Veldhoven Formation in section D–D′ (Figure 8). The thickness of the Voort Member on section D–D′ changes abruptly several times across faults belonging to the Veldhoven Fault System. These changes in thickness become less towards the top of the Veldhoven Formation

and faults terminate in the Wintelre Member. The Voort Member is thickest in the southern part of the RVG (Figure 5). Here, the lower part of the member shows north-westward progradation as inferred from the slightly inclined reflections (<1°) downlapping the base of the Veldhoven Formation and becomes very thin towards the north-west. The upper part of the member displays aggradation, as observed from the parallel stacking of reflectors in a symmetrical pattern. Reflection amplitudes in the upper part can vary laterally, which may be signified as a facies transition. An example occurs around well Heel, where high-amplitude reflections laterally fade (Figure 5). The top of the Voort Member also shows a distinct increase in reflection amplitudes near well Heel (Figure 5). This may indicate a change in facies from marine sand to more heterogenous sand–clay alternating deposits, announcing the transition towards the Wintelre Member. Compared to the overlying Wintelre and Someren members of the Veldhoven Formation, the Voort Member shows lower-amplitude and lower-frequency reflections, highlighting a more homogenous composition of the sediment. The top of the Voort Member is picked at a soft-kick (red) reflection.

4.2.1.2 | *Wintelre Member*

The Wintelre Member is recognized on seismic sections by variable-frequency and variable-amplitude reflections with a relatively high continuity. The unit is present in the RVG and is thickest along the central axis of the southern and central RVG (Figure 7). The base of the Wintelre Member is picked on a hard-kick (blue) reflection, whereas the top is picked on a soft-kick (red) reflection. The Wintelre Member shows parallel reflectivity on top of the Voort Member on seismic sections oriented SE-NW (Figures 5 and 8) but shows onlap features against the rims of the RVG on sections oriented SW-NE (Figures 6 and 7). The unit displays a variable thickness along the southern rim of the RVG on section D–D′ (Figure 8) and tends to disappear towards the north-west from what can be observed on seismic sections. Reflection amplitudes vary laterally throughout the study area and tend to be higher along the southern rim of the RVG (Figure 8) compared to the northern RVG (Figure 5), whereas reflection frequencies tend to be higher in the northern RVG. This may be an effect of lithological changes within the Wintelre Member and is confirmed by lithological descriptions that mention a much more sand-rich interval with silty clay intervals in wells HVB-01, compared to very plastic homogenous clay in well SMG-01. The top of the Wintelre Member is a conformable surface and does not feature any clear signs of erosion, such as channel incisions or truncation through reflector termination.

4.2.1.3 | *Someren Member*

The Someren Member has similar seismic characteristics as the Wintelre Member, such as a relatively high continuity and variable reflectivity, but exhibits slightly higher-amplitude reflections in the Someren Member in the northern RVG (Figures 5 and 6). This trend is opposite in the southern part of the RVG and along its southern rim, where the Wintelre Member exhibits higher-amplitude reflections (Figures 7 and 8). A regional change in facies across the Someren Member is plausible.

Lithological descriptions from well SMG-01 in the northern RVG describe dark grey–greenish clay that is very plastic and glauconite rich (see above). The same description is noted for the underlying Wintelre Member here, explaining the similarity in seismic characteristics. In well HVB-01 located along the southern rim of the RVG, the amount of sand increases and molluscs appear towards the top of the formation, which we assign to the Someren Member. The underlying Wintelre and Voort members are glauconitic light-grey to grey-green clays interbedded with silt and sand, explaining the higher variability in reflection amplitudes observed on seismic sections (Figures 6 and 8). The trends described in well HVB-01 were also observed on the Belgian side of the RVRS. Deckers (2016) described a strongly reflective Veldhoven clay (Belgian Wintelre equivalent), and a weakly reflective Someren Member. Hence, the southern rim and south-eastern part of the RVRS display a relatively homogenous sand-rich Someren Member that transitions into a more heterogenous clay-rich unit with frequent sand and silt intercalations in the central part of the RVG during the same period that resembles the Wintelre Member facies more. The clay-rich facies of the Someren Member in the central RVG is more likely a deeper-marine, distal equivalent of the more shallow-marine, sand-rich Someren Member found along the southern rim and south-eastern part of the RVG. The underlying Wintelre Member, described by Munsterman and Deckers (2022) in the south-eastern part of the RVG as a restricted marine facies, rather precedes the clay-rich interval found in the central part of the RVG. The lithological heterogeneity of the Someren Member towards the central RVG may be partly attributed to mass transport complexes (MTCs) that originate from the west. Seismic sections oriented SE–NW through the centre of the RVG (Figure 5) exhibit chaotic, high-amplitude, high-frequency reflections along the slope of the southern RVG (SF11 – Table 2). The top of the Veldhoven Formation is marked by the EMU (Figure 2). It appears as a generally high-amplitude, variable-frequency reflection, represented by a hard-kick (blue) along the rims of the RVG, and a soft-kick (red) reflection in the deeper parts of the RVG (Table 1). Low-angle truncations and gully incisions

are observed in the north-westernmost part of the RVG on section A–A′ (Figure 5) and along the southern rim of the RVG on section D–D′ (Figure 8). In the northern part of the RVG, no clear signs of erosion are observed. Locating the EMU on seismic data can be challenging since an onlap surface or erosional truncation is not always present. To determine EMU correlations, we therefore rely on palynologically determined ages and cross-correlations between different seismic sections.

4.2.2 | Seismic characteristics of the Groote Heide Formation

The distribution of the Groote Heide Formation has been mapped through 2D seismic interpretation of the EMU and MMU throughout the RVRS (Figure 9a,b). Thickness distribution maps reveal that the main depocentre is located in the southern part of the RVG and along the Peel Boundary Fault System, where a maximum thickness of about 390 m is inferred (Figure 9d). Preservation on the Peel Block is variable, which is partly caused by uncertainty in the interpretation due to the occurrence of many faults, lack of well data and low seismic quality in the shallow subsurface. Seismic interpretations on the Peel Block show an estimated thickness range between 0 and 185 m, with an average of about 60 m. On the Venlo Block, the formation ranges between 20 and 200 m and gradually thickens towards the north-west. The average thickness of the Venlo Block is about 130 m. The Groote Heide Formation becomes considerably thinner across the Veldhoven Fault System on the Campine Block, particularly in the west. Similar to the Peel Block, seismic data are limited here due to its bad quality in the shallow subsurface. We estimate a range between 0 and 110 m, with an average of about 45 m. A total sedimentary volume in the Groote Heide Formation of 934 km^3 was estimated.

4.2.2.1 | *Kakert Member*

The Kakert Member is characterized by high-amplitude, high-frequency reflections with a strong continuity that can be traced along a wide area within the RVG (SF10, Table 2). This observation is consistent with observations from Deckers (2015) regarding the Houthalen Member; the Belgian equivalent of the Dutch Kakert Member (Figure 2). Some reflectors show low-angle onlap on the EMU towards the south-east (Figure 5) or onlap the southern margin of the RVG towards the south-west (Figures 6 and 7), illustrative for a transgressional phase. Its upper boundary is marked by a high-amplitude, hard-kick reflection, where the Heksenberg Member lies conformably on top of the Kakert Member. The Kakert Member is relatively thin, ranging between 5 and 45 metres in the RVG, based on both well and seismic interpretations.

4.2.2.2 | *Heksenberg Member*

The Heksenberg Member has a thickness ranging between 0 and 113 m and is confined to the south-eastern part of the RVRS. Towards the north-west, the marine influence increases and the Groote Heide Formation becomes more homogenous. As mentioned before, the members are therefore lumped together as the Rucphen Member in the northern RVG (Figure 2). The Heksenberg Member is recognized on seismic sections by the presence of lignite beds characterized by high-amplitude, (soft-kick), low-frequency, rugged reflections that thin towards the north-west (SF9, Table 2). Small faults are observed through the offset between reflectors. The high-amplitude reflections associated with the presence of lignite seams in the south-eastern part of the RVG are best visible in section A–A′ (Figure 5). However, they do not always represent lignite. As inferred from well data in Roermond and Heel, the highly reflective layers also correspond to frequently alternating beds of sand and silt/clay that can be more or less humic. The Heksenberg Member loses its characteristic seismic reflection towards the north-west, where the reflection amplitudes decrease due to the absence of sand–lignite alternations (Figure 5). Within the Heksenberg Member, north-westward progradation of low-angle clinoforms (0.7–1.2°) with foreset heights of approximately 20 m is observed in continuation of the lignite seams in the south-east. These clinoforms are present in the southern part of the RVG, north-west of well NDW-01 and south-east of well Heel (Figure 5). The clinoforms south-east of well Heel are located directly in front of the lignite-rich beds, likely representing shallow-marine coastal clinoforms. These clinoforms have foreset heights of 30–45 m with a dip of 0.5–1.5°. Towards the north-west, the unit transitions into the fully marine Rucphen Member.

4.2.2.3 | *Vrijherenberg Member*

The Vrijherenberg Member is characterized by variable-amplitude, continuous parallel reflections with dim patches that show an aggradational pattern (SF 8, Table 2) in the south-eastern part of section A–A′ (Figure 5). The lower boundary of the Vrijherenberg Member is picked on a peak (red reflection) and represents a conformable downlap surface on the top of the Heksenberg Member (Figure 5) and an onlap surface against the southern rim of the RVG (Figure 7). The upper boundary is picked on a peak (red) and marked by incised valleys or an irregular rough subparallel surface in the southern part of the RVG. Towards the northern RVG, the upper boundary is formed by a conformable downlap surface for the

overlying Diessen Formation with north-westward dipping reflectors. The Vrijherenberg Member is thickest in the south-eastern RVRS, around well NDW-01 and rapidly thins towards the north-west and along the northern and southern rims of the RVG. In the southern RVG, shingled clinoforms start to develop around well NDW-01 that prograde in north-western direction (Figure 10). Foreset heights range between 20 and 60 ms TWT (approximately 15–55 m) and foreset dips between 1 and 1.2° (SF3, Table 2). Clinoforms in the Vrijherenberg Member are located further north-westward compared to those in the Heksenberg Member, indicating overall progradation of the Groote Heide Formation in the same direction over time. Interestingly, they only seem to occur in the lower part of the member, below the maximum flooding surface (MFS) mentioned before in section 4.1.2. Towards the north-west, the typical clinoform geometry disappears and toesets gently downlap the underlying surface at a very low angle. As mentioned before, the Vrijherenberg Member transitions into the Rucphen Member towards the northern RVG. The Rucphen Member tapers towards the basin margins, onlapping the underlying topography (Figure 6), and shows much higher reflectivity, especially in its upper part (Figures 5 and 6). This contrasts with the southern RVG, where the lower part of the Groote Heide Formation, containing the Kakert Member or Heksenberg Member, shows higher reflectivity than the upper part containing the Vrijherenberg Member. The top of the Vrijherenberg Member, which is also the top of the Groote Heide Formation, is marked by a surface associated with the MMU. We pick the MMU on a high-amplitude peak (red) reflection signifying a downlap surface across the study area (Table 1). This is most evident in seismic section B–B′ (Figure 6). Indications for erosion related to the MMU are observed in the southern RVG and on the Peel Block. Along section A–A′ near well NDW-01 (Figure 5), deep incisions of up to around 75 ms TWT are present in the upper part of the Vrijherenberg Member. These incised valleys appear to be oriented perpendicular to the seismic section, implying a SW–NE flow direction. In section B–B′, a large V-shaped feature with a vertical scale of 200 ms TWT is visible on the Peel Block around the interpreted MMU surface (Figure 6). In section C–C′ (Figure 7), the MMU is picked on a rugged reflection, possibly denoting an erosional surface as well. Section D–D′ (Figure 8) depicts a very thin Groote Heide Formation along the southern margin of the RVG but does not reveal any further seismic features that could evidence an unconformity. These remnants of an erosional phase may well be linked chronologically to the 'Diest gully' on the Campine Block in the south. This erosional incised depression is recorded at the base of the Belgian Diest Formation (Diessen Formation) and is described by Deckers and Louwye (2019), Houthuys et al. (2020) and Vandenberghe et al. (1998, 2014). The associated hiatus spans somewhere between 13.8 and 11.6 Ma and is related to subsidence of the RVG and uplift of the Brabant Massif (Louwye et al., 2007; Vandenberghe et al., 2014).

4.2.3 | Seismic characteristics of the Diessen Formation

The late Miocene Diessen Formation is characterized by the widespread occurrence of clinoforms, generally prograding from the south-east towards the north-west. Seismic data reveal reflections with overall low amplitudes compared to the subjacent Groote Heide Formation and superjacent Oosterhout or Kieseloolite Formation. The base of the Diessen Formation represents a downlap surface in the northern RVG, where clinoform toesets downlap and onlap the underlying topography represented by the MMU (Figure 6). The formation is characterized by seismic facies SF3-7 (Table 2). SF3 is represented by high-frequency, medium-amplitude reflections that reveal oblique and sigmoidal-shaped clinoforms that are mainly present in the southern RVG. SF4 and SF5 represent larger-scale clinoforms that are observed in the northern RVG. SF6 and SF7 are individual features observed in the Diessen Formation.

The distribution of the Diessen Formation has been mapped through 2D seismic interpretation of the MMU and LMU throughout the RVRS, resulting in regionally interpolated surfaces that reveal their current depth (Figure 9b,c). The resulting thickness distribution map indicates that the main depocentre was located in the northern RVG during the late Miocene, where a maximum thickness of about 645 m is inferred. Seismic image quality of the Diessen Formation is low on the Peel Block, but combined with well correlations we estimate a thickness varying between 0 and 160 m, with an average of 46 m. On the Venlo Block, the formation ranges between 3 and 265 m where it gradually thickens towards the north-west. An average thickness of 98 m is estimated here. Towards the Campine Block, across the Veldhoven Fault System, the thickness of the Diessen Formation gradually declines. On the Campine Block and in the north-westmost part of the RVG, the Diessen Formation is relatively thin, but its thickness increases towards the south-east. Seismic data are limited here, but interpretations suggest a thickness range of 0–135 m, with an average of 55 m. Overall, we observe a shift of the main depocentre towards the north-west from the early–middle Miocene to the late Miocene. Additionally, the depocentre becomes narrower in the late Miocene and a gradual shift of the clinoform complex towards the Veldhoven Fault is observed. This

roughly follows the north-west to west-south-westward progradation direction of clinoforms within the Diessen Formation. The total sedimentary volume in the Diessen Formation is estimated at about 1364 km^3, compared to 934 km^3 for the Groote Heide Formation, although the depositional period of both formations is similar.

Clinoforms are characteristic of the Diessen Formation and have a much more widespread occurrence than the ones in the Vrijherenberg and Heksenberg members. Across the RVG, foreset heights vary from about 50 m in the southern RVG (Figures 5 and 7), dipping between 1 and 2°, to about 200 m in the northern RVG, dipping between 2 and 6° (Figures 6 and 8). The latter falls somewhere in between delta-scale and shelf-edge clinoforms in terms of relief and foreset slope. According to Patruno and Helland-Hansen (2018), delta-scale clinoforms are characterized by 3–50 m of relief and a delta slope of <27°, whereas shelf-edge clinoforms correspond to 100–300 m of relief, delta slopes of 0.6–4.8° and a much larger downdip extent (Patruno et al., 2015; Steel & Olsen, 2002). Variation in clinoform geometry occurs between the Diessen subunits. Clinoforms in subunits Diessen-A and -D have the lowest foreset angle and passively drape the underlying surface, without much variation between foreset and toeset thickness (Figures 5 and 8). These features are most prominent in subunit Diessen-A. Meanwhile, progressively steepening clinoform foresets are found in subunits Diessen-B and -C along the Veldhoven Fault System, where more contrast exists between foreset and toeset thickness (Figure 8). Clinoform trajectories indicating (pseudo) directions of progradation have been mapped on 19 2D seismic sections and are each designated to one of the Diessen subunits (Figure 10). Two changes in the direction of progradation have been observed. Clinoforms in subunits Diessen-A and -B show an overall west-to-north-west direction of progradation, suggesting a north–north-east- to south–south-west-oriented palaeocoastline. Clinoform progradation in subunit Diessen-C tends to be rotated counterclockwise towards the west-south-west (Figure 10). Only along the Veldhoven Fault System, clinoforms prograde towards the north-west (Figure 8). Subunit Diessen-D shows a clockwise rotation in clinoform progradation again towards the north-west along the Veldhoven Fault System (Figures 8 and 10). This trend continues into the Pliocene.

4.2.3.1 | *Diessen-A*

Subunit Diessen-A is characterized by variable-amplitude, medium-frequency reflections. The geometry indicates progressive fill of the RVG from the centre towards its margins (Figures 6 and 8). On section B–B′ (Figure 6), in the northern RVG, subunit Diessen-A thins towards the south-west where it gently drapes the underlying topography. Clinoforms in subunit Diessen-A have very low-slope gradients and a long down-dip extent throughout the area. Around the clinoform, toesets reflections show increased amplitudes, for example, on section B–B′ (Figure 6). This could be a consequence of either sand–clay alternations on a short scale or due to thin-bed tuning effects (Whitcombe, 2002) caused by constructive interference from overlapping seismic reflections. In section C–C′ (Figure 7), subunit Diessen-A exhibits rapid thickening towards the Peel Boundary Fault System. SE–NW-oriented sections A–A′ and D–D′ (Figures 5 and 8) show progressive thickening of subunit Diessen-A towards the south-east. Seismic interpretations infer a thickness ranging between 5 and 130 m, where subunit Diessen-A is thickest in the central RVG and tapers towards the north-west and the Campine Block. Observations indicate that the main depocentre of subunit Diessen-A was situated in the central RVG along the Peel Boundary Fault System (PBFS). Thickness differences across faults only seem to be affected by faults in the PBFS, but not by the Veldhoven Fault System. Along the PBFS, the footwall and hanging wall highlight major changes in thickness across the fault, with a maximum vertical throw of about 130 ms TWT (roughly 120 m) as observed on seismic section C–C′ (Figure 7). Along the Veldhoven Fault System, the thinning effect towards the Campine Block is very gradual, showing no major thickness variations across faults. Interestingly, subunit Diessen-A is thickest around well NDW-01 in the central RVG, while situated on a currently anticlinal feature. This suggests folding took place during a later phase, where the direction of compression must have roughly been SE–NW oriented.

4.2.3.2 | *Diessen-B*

Subunit Diessen-B is characterized by the extensive occurrence of clinoforms in the RVG that prograde towards the west-north-west (Figures 5, 8, 10). Clinoforms start developing in the central part of the RVG, north-west of well NDW-01 (Figure 5). Transect B–B′ reveals progressive infill of the northern RVG by subunit Diessen-B from north-east to south-west (Figure 6), resulting in a thicker sequence near the Peel Boundary Fault System compared to the area near the Veldhoven Fault. Interpreted clinoform trajectories on 2D seismic sections (Figure 10) indicate variable progradation directions in subunit Diessen-B, ranging between north-west and south-west. Furthermore, the size of clinoforms and their stacking patterns seem to be divided into two units, best observed on section C–C′ (Figure 7). The lower part of subunit Diessen-B shows westward prograding clinoforms with foreset height of about 50–70 m that onlap the underlying topography towards the southern rim of the RVG. The upper part of subunit Diessen-B becomes much

thicker towards the Veldhoven Fault System, showing stacking patterns that are likely initiated by tectonic activity. This subdivision is expressed on seismic sections A–A′ (Figure 5) and B–B′ (Figure 7) as a lower part of Diessen-B reflecting a relatively even thickness throughout the area where clinoforms in the central and northern RVG are draping the underlying surface, and an upper part of Diessen-B becomes a lot thicker, especially in the clinoform foresets. The overall high lateral continuity of clinoform sets in subunit Diessen-B may be indicative of external control on accommodating the fluvio-deltaic system, such as tectonics and/or climate. The upper boundary of subunit Diessen-B corresponds to the base of the emerging Inden Formation within the RVG (Figure 6).

4.2.3.3 | *Diessen-C*

Subunit Diessen-C is thinly distributed in the southern RVG as it transitions into the Inden Formation here. The Inden Formation represents the proximal time equivalent of subunit Diessen-C in the central and southern parts of the RVG (Figure 2). The distal marine facies represented by subunit Diessen-C, however, rapidly thickens towards the northern RVG and its southern rim. Transect B–B′ (Figure 6) demonstrates progressive north-east to south-west infill of the northern RVG. Along the southern rim of the RVG, north-westward clinoform progradation is observed with gradually steepening clinoform foresets in the same direction (section D–D′, Figure 8). The internal reflectivity is generally dim but shows high-amplitude toesets and bright reflections at the boundaries between certain clinothems. Topsets are often limited in their extent. Inflection points towards the foresets can be observed on sections A–A′ and C–C′ (Figures 5 and 7), but clearly much more sediment is preserved in the foreset, indicating that progradation of the system is more dominant than aggradation. Either vertical accommodation space was limited or long-shore transport played an important role in the distribution of sediment. There are no indications for erosion or subaerial exposure within Diessen-C as observed from wells in the central part of the RVG (e.g. wells HVB-01 and SMG-01). In section B–B′ (Figure 6) and D–D′ (Figure 8), three phases of clinoform progradation can be distinguished within subunit Diessen-C, separated by high-amplitude reflections against which the clinoform topsets of the underlying clinothem truncate. In sections B–B′ (Figure 6) and D–D′ (Figure 8), topsets of subunit Diessen-C truncate against the Kieseloolite Formation in the south-eastern parts of the section, lining up with the development of the LMU.

4.2.3.4 | *Diessen-D*

Subunit Diessen-D is represented on seismic sections as west-north-westward prograding clinoforms and can only be observed in sections B–B′ and D–D′ along the southern margin of the Roer Valley Graben (Figures 6 and 8). Clinoforms include foresets and toesets, but topsets are only visible for the south-eastern part of Diessen-D on section D–D′ (Figure 8). Towards the north-west, the unit drapes the underlying surface, and a clear distinction between foreset and topset is not easily made. Reflection amplitudes and frequencies are highly variable. In section B–B′, a maximum thickness for subunit Diessen-D of about 110 m is observed between boreholes BKZ-01 and HVB-01 (Figure 6). The base of subunit Diessen-D is characterized by high-amplitude reflections against which reflectors of the underlying Diessen-C subunit truncate, and above which reflectors of the overlying Oosterhout Formation onlap to the east, suggesting an erosional unconformity at the top of subunit Diessen-D. In section D–D′, the base of subunit Diessen-D follows the underlying topography. The top of subunit Diessen-D aligns with the LMU.

The LMU is identified by a low-amplitude reflection, in some areas associated with truncation of the underlying Diessen Formation clinoforms (Table 1). This is most pronounced in section D–D′ (Figure 8), where topsets of subunits Diessen-B, -C and -D are truncated along the southern margin of the RVG. No truncation is observed on seismic sections along the central axis of the RVG, where the Oosterhout Formation conformably overlies the Diessen Formation. As described in previous sections, well logs and biostratigraphy results revealed progressive shallowing from the late Miocene into the Pliocene. In the north-westernmost part of section A–A′ (Figure 5), reflectors of the Diessen Formation either truncate against the LMU at a very low angle or alternatively, thin out towards the north-western rim of the RVG. On top of the LMU, clinoforms from the Oosterhout Formation clearly downlap the LMU towards the north-west.

4.2.4 | Seismic characteristics of the Kieseloolite Formation and Oosterhout Formation

The Kieseloolite- and Oosterhout formations, representing late Miocene–Pliocene deposits, overlie the Diessen Formation (Figure 2). The Kieseloolite Formation is present in the south-eastern RVRS, while the Oosterhout Formation, its marine counterpart, occurs in the northern and north-western RVRS.

The Kieseloolite Formation is characterized by semi-continuous reflections of variable amplitude that are interpreted as channel incisions (SF1, Table 2). Bright reflections abruptly end and show a limited continuity. The bedding is largely horizontal or follows the underlying

topography. Towards the north-west, onlap and downlap features start to develop, and the internal architecture becomes somewhat chaotic as the Kieseloolite Formation appears to transition into the Oosterhout Formation. Further north-west, the continuity of reflections becomes better, and their frequency becomes lower. In general, the Oosterhout Formation is characterized by low-amplitude, low-angle dipping reflections that downlap onto the LMU (SF2, Table 2). However, in the north-westernmost part of the RVG, high-angle clinoforms prograde towards the north-west just above the LMU (section A–A′, Figure 5).

5 | SEQUENCE STRATIGRAPHIC INTERPRETATIONS AND IMPLICATIONS

Below we outline the sequence stratigraphic interpretation based on seismostratigraphic architecture, facies analysis and well data. Sequence stratigraphic features in the Miocene sequence are best observed between the southern and central RVG. We therefore use part of the seismic section in Figure 5 to illustrate the sequence stratigraphy in Figure 11.

The early Miocene unconformity (EMU) at the base of the marine Kakert member is formed by a maximum regression surface (MRS 1), followed by a transgression. After the following maximum flooding surface (MFS 1), the depositional system of the Kakert Member gradually shallows and is marked at the top by MRS 2 around the transition between the Kakert Member and Heksenberg Member (Figure 11). The MRS is followed by a transgression, corresponding to the Frimmersdorf Sand, with the maximum transgression indicated by MFS 2. A Highstand Systems Tract (HST) follows that matches with Biozone M6 (well NDW-01, Figure 11). The common presence of the dinoflagellate cyst species *Polysphaeridium zoharyi* and *Paralecaniella* spp. in Biozone M6 (well NDW-01) in the Heksenberg Member points to a coastal to shallow marine (restricted) environment. A relatively distal (shallow marine) setting seems likely since sporomorphs are not represented in large numbers. Following the maximum regression (MRS 3) in the upper part of Biozone M6, a base level rise marked by a transgressive systems tract (TST) occurs above a sampled record of Biozone M6, marked at the top by MFS 3. Subsequently, a shallowing upward follows during highstand progradation (HST) and consecutive falling stage systems tract (FSST). This is inferred from aggradating clinoforms north-west of well NDW-01 (Figure 11) and subsequent downstepping of clinoforms observed from the rollover points between topsets and foresets. MRS 4 marks the top of the Heksenberg Member. The marine Vrijherenberg Member starts with a base level rise, marked by a TST and HST. The TST sequence in the Vrijherenberg Member is quite thick. Often, the transgressive sequence is thin but higher than normal sedimentation rates and rapid base level rise can cause thicker preservation. Since the global sea level curve does not change rapidly during this period (Figure 2) (Miller et al., 2005), this suggests the involvement of a tectonic component to create space for sediment accumulation. An MFS (MFS 4) can be recognized as a high-amplitude blue reflection around the middle of the Vrijherenberg Member and as a sharp decrease in travel time on the sonic log (Figure 11). The MFS surface in the Vrijherenberg Member was also interpreted by Deckers and Munsterman (2020) and Munsterman et al. (2019) in the RVG and by Prinz et al. (2017) in the Lower Rhine Graben. In the RVG, these authors inferred maximum-gamma-ray values coinciding with the most glauconite-rich part of the Vrijherenberg Member, and a maximum number of open-marine dinocysts in a condensed interval comprising Biozones M8-10. In the Lower Rhine Graben, Prinz et al. (2017) described a maximum transgression in the Neurath Sands (Figure 2) around the middle Serravalian. A Serravalian transgression was also described by Rasmussen et al. (2010), Rasmussen and Dybkjær (2014) and Thöle et al. (2014) in the eastern North Sea Basin, inferred by a condensed section of glauconite-rich mud and was attributed to a relative sea-level rise driven by increased subsidence of the North Sea Basin. Above the MFS, a relatively thick HST develops as seismic reflectors reveal parallel aggradation within the sequence. The top of the Vrijherenberg Member is marked by the MMU. In this part of the RVRS, we interpret the MMU as a basal surface of forced regression, resulting from an FSST that caused deep incisions into the Vrijherenberg Member that go as deep as the MFS. Possibly the erosive-resistant clay at this level prohibited/hampered further incision here. In the deeper parts of the RVG, no such incisions were observed, and sedimentation is believed to have been continuous here. Palynological analyses from Biozone M11 in well NDW-01 indicate that dinoflagellate cysts diminish both in species abundance and in numbers, indicating regression. This period coincides with the Serravallian–Tortonian transition, during which a large global sea-level drop took place (Haq et al., 1987; Hardenbol et al., 1998; Kominz et al., 2008; Miller et al., 2005) (Figure 2). This may explain the deep incisions associated with the MMU. Due to the incision, the FSST was not preserved. The incised valley fill is linked to an LST that was deposited during the latest Serravallian–early Tortonian and belongs to Diessen-A. Incised valley fills related to an LST are more commonly observed (Rasmussen, 2014),

and are well-known in Pleistocene successions (e.g. Wang et al., 2020). The incised valley fill is not observed everywhere. In most parts of the RVG, the marine sands of Diessen-A transgress over MRS 5 (Figure 11) towards the south-east. This TST is followed by a relatively thin HST, as displayed by a uniformly thick layer in the top of subunit Diessen-A that is recognized in other wells as an aggrading pattern on the gamma-ray log. A renewed phase of transgression marks the lower part of subunit Diessen-B, where clinoforms onlap the top of subunit Diessen-A towards the south-east. The middle part of subunit Diessen-B is marked by an FSST and subsequent LST, as evidenced by downstepping clinoforms, which can be better observed in Figure 5. Despite the regression within subunit Diessen-B, a fully marine environment is still evidenced as Dinoflagellate cysts from Biozone M12 have an abundance of the open marine species *Spiniferites* spp. Another transgression follows, where the MFS marks the base of subunit Diessen-C. An HST follows, as interpreted from the parallel, horizontal aggradation of seismic reflectors. The boundaries and sequence stratigraphic context among subunit Diessen-C, the Inden Formation and the Oosterhout Formation is ambiguous since the inferred Piacenzian, or older, and early Zanclean, or older, ages are uncertain. The marine influence is still clear for the early Zanclean or older sample, but the presence of the taxon *Operculodinium* spp. may indicate changing conditions (e.g. temperature and salinity) from a marine environment (Diessen Formation) into a fluvial environment (Inden Formation). The overlying Piacenzian or older sample shows an abundance of woody and other plant fragments, as well as a dominance of bisaccates (type of pollen), suggesting a near-coastal setting.

If we link the interpreted sequence stratigraphic surfaces and adhering systems tracts to the Miller sea level curve shown in Figure 2, the Kakert Member and Heksenberg Member seem to follow the global sea level fluctuations of Miller et al. (2005) quite well, but from the Vrijherenberg Member onwards, the sedimentary sequence is defined mostly by alternating HSTs and TSTs (except for Diessen-B), while global sea levels have dropped between the MMCO and MMCT and remained relatively stable (Figure 2). We therefore argue that tectonic subsidence must have played a role in creating accommodation. The MMU and associated regression causing the incised valley in Figure 11 can be linked to a severe global sea level drop around 11 Ma (Haq et al., 1987; Kominz et al., 2008; Miller et al., 2005). The sequence stratigraphic features in the Roer Valley Graben can be linked to the Belgian Miocene sequence. The members in the Groote Heide Formation have been correlated well in literature (e.g. Deckers & Louwye, 2019; Deckers & Munsterman, 2020), but no attempt has yet been made to correlate the different members within the Belgian Diest Formation to the Dutch Diessen Formation. We therefore propose that subunit Diessen-A can be correlated with (the lower part of) the Belgian Dessel Member. It was proposed by Vandenberghe et al. (2014) that the Dessel Member can be attributed to a shallow, low-energy transgression during the early Tortonian, depositing a relatively thin fine-grained layer of sediment (Houthuys, 2014; Vandenberghe et al., 2005). We correlate subunit Diessen-B to the Belgian Hageland Diest Member in the eastern Campine Block. In the western Campine Block, the unit chronologically corresponds to the Deurne Member and upper part of the Dessel member. The age of the Hageland Diest Member is uncertain since the sand is microfossil barren, but literature (e.g. Houthuys, 2014; Houthuys et al., 2020; Vandenberghe et al., 2014) suggests it is coeval with the early-to-middle Tortonian. The Hageland Diest Member is interpreted as a near-coastal continental shelf, built of medium-to-coarse glauconitic sand, with NE-dipping foresets in metres-thick cross-beds (Vandenberghe et al., 2014). Houthuys (2011) interpreted the unit to be the strong-current fill of narrow, elongate flow channels. The driving mechanism for near-simultaneous erosion and fill is argued to be continuous external sand supply by a coastal pathway under highstand conditions into a semi-enclosed embayment situated over the Campine, and tributary to the marine RVG. Subunit Diessen-C may be correlated with the Kempen Diest Member of late Tortonian age and is related to Biozones M14 and M15. The member is described as a single, large marine delta prograding from SE to NW (Houthuys et al., 2020). We also observe these features in section D–D′ in subunit Diessen-C along the Veldhoven Fault System. Houthuys et al. (2020) also state that the Kempen Diest sand is the lateral equivalent of the fluviatile Inden Formation in the Lower Rhine Basin, inferred from the angular fluvial-derived coarse-sand grains and a significant fraction of weathered continental clay minerals mixed throughout the Kempen Diest sand. In this work, subunit Diessen-C is also referred to as the distal counterpart of the Inden Formation in the RVG (see Sections 4.1.3 and 4.2.3). The top of the Kempen Diest Member is clayey glauconitic sand that is characterized by the unusual presence of Fe-vermiculite derived from altered glauconite-bearing soil, representing subaerial exposure (Adriaens et al., 2020). This marks the boundary between the Belgian Kempen Diest Member and the Kasterlee Formation, which we correlate in this study to the transition

between subunits Diessen-C and Diessen-D (Figure 2). The Kasterlee Formation is described as a sublittoral facies that was deposited in a somewhat shallower marine environment than the Belgian Diest Formation. In the RVG, subunit Diessen-D is characterized by the lowest gamma-ray values in the Diessen Formation, indicating the presence of coarser material and/or less glauconite, likely pointing to a shallower environment as well. The regional correlation of the Dutch Miocene succession to the Belgian and German stratigraphy (Figure 2) in a sequence stratigraphic context points out that not only local tectonics controlled the basin infill, but a more regional/eustatic control played its part as well.

6 | CONCLUSIONS

Well logs, lithological descriptions and dinoflagellate cyst palynology were used to characterize the depositional units in the Miocene sequence of the Roer Valley Rift System (RVRS). 2D seismic sections were used to further infer lithological trends, stratal patterns and unconformities. Combined, they indicate the migration of depocentres and evolution of sediment supply.

1. The main depocentre in the central Roer Valley Graben shifts from the south-east in the early and middle Miocene towards the north-west in the late Miocene. In addition, the Roer Valley Graben gradually fills from the Peel Boundary Fault System towards the Veldhoven Fault System over the Miocene period.
2. The overall direction of clinoform progradation was to the west-north-west during the middle Burdigalian–Serravallian. It gradually shifts counterclockwise to the west-south-west during the late Serravallian–Tortonian. A final shift back in clockwise direction to the north-west occurs during the late Tortonian and Messinian.
3. The Diessen Formation can be subdivided into four units, each marked by a renewed phase of progradation. The subunits can be correlated to the regional German and Belgian stratigraphy where similar sequence stratigraphic patterns are observed.
4. Three major unconformities are present in the study area, namely the early, middle and late Miocene unconformities (EMU, MMU and LMU). The MMU has had the most impact on the structural highs surrounding the southern RVG, the Peel Block and the Campine Block, where several large incisions are observed on seismic sections, and a hiatus comprising the Serravallian–early Tortonian is recorded. In the central and northern RVG, the MMU is not related to an erosional hiatus and sedimentation is continuous.

ACKNOWLEDGEMENTS

We would like to thank Geological Survey of the Netherlands (TNO-GDN) for funding this project and the opportunity to use their extensive database. Furthermore, we are grateful to Schlumberger for granting us a free licence for Petrel®.

PEER REVIEW

The peer review history for this article is available at https://www.webofscience.com/api/gateway/wos/peer-review/10.1111/bre.12886.

DATA AVAILABILITY STATEMENT

The data that support the findings of this study are available from the corresponding author upon reasonable request.

ORCID

Alexandra Siebels https://orcid.org/0009-0004-8883-8015

REFERENCES

Adriaens, R., & Vandenberghe, N. (2020). Quantitative clay mineralogy as a tool for lithostratigraphy of Neogene Formations in Belgium: A reconnaissance study. *Geologica Belgica*, *23*(3–4), 365–378.

Boenigk, W., & Frechen, M. (2006). The Pliocene and Quaternary fluvial archives of the Rhine system. *Quaternary Science Reviews*, *25*(5), 550–574.

Böhme, M. (2003). The Miocene Climatic Optimum: Evidence from ectothermic vertebrates of Central Europe. *Palaeogeography, Palaeoclimatology, Palaeoecology*, *195*(3), 389–401.

Böhme, M., Aiglstorfer, M., Uhl, D., & Kullmer, O. (2012). The Antiquity of the Rhine River: Stratigraphic Coverage of the Dinotheriensande (Eppelsheim Formation) of the Mainz Basin (Germany). *PLoS One*, *7*(5), e36817.

Camelbeeck, T., & Eck, T. (1994). The Roer Valley Graben earthquake of 13 April 1992 and its seismotectonic setting. *Terra Nova*, *6*(3), 291–300.

Cameron, T., Crosby, A., Balson, P., Jeffery, D., Lott, G., Bulat, J., & Harrison, D. (1992). *The geology of the southern North Sea United Kingdom offshore regional report*. British Geological Survey and HMSO.

Catuneanu, O. (2006). Principles of sequence stratigraphy. In *Developments in sedimentology* (p. 58). Elsevier.

Catuneanu, O., Galloway, W. E., Kendall, C. G. S. C., Miall, A. D., Posamentier, H. W., Strasser, A., & Tucker, M. E. (2011). Sequence stratigraphy: Methodology and nomenclature. *Newsletters on Stratigraphy*, *44*(3), 173–245.

De Bruin, G., Geel, K., Houben, S., Munsterman, D., Verweij, H., Smit, J., Janssen, N., Kerstholt-Boegehold, S., & Vandeweijer, V. (2015). MMU—Unravelling the stratigraphic and structural development of the strata found underneath and above the mid-Miocene unconformity. *TNO Report*, *2015*, R10425.

De Schepper, S., Head, M., & Louwye, S. (2004). New dinoflagellate cyst and incertae sedis taxa from the Pliocene of Northern Belgium, Southern North Sea Basin. *Journal of Paleontology*, *78*, 625–644.

De Verteuil, L., & Norris, G. (1996). Miocene dinoflagellate stratigraphy and systematics of Maryland and Virginia. *Micropaleontology*, *42*, i–viii.

Deckers, J. (2015). Middle Miocene mass transport deposits in the southern part of the Roer Valley Graben. *Marine and Petroleum Geology*, *66*, 653–659.

Deckers, J. (2016). The Late Oligocene to Early Miocene early evolution of rifting in the south-western part of the Roer Valley Graben. *International Journal of Earth Sciences*, *105*, 1233–1243.

Deckers, J., & Louwye, S. (2019). A reinterpretation of the ages and depositional environments of the lower and middle Miocene stratigraphic records in a key area along the southern margin of the North Sea Basin. *Geological Magazine*, *156*(3), 525–532.

Deckers, J., & Munsterman, D. (2020). Middle Miocene depositional evolution of the central Roer Valley Rift System. *Geological Journal*, *55*(9), 6188–6197.

Demyttenaere, R. (1989). The post-Paleozoic geological history of north-eastern Belgium. *Letteren en Schone Kunsten van België*, *51*, 51–81.

Doornenbal, J. C., & Stevenson, A. G. (Eds.). (2010). *Petroleum geological atlas of the southern Permian Basin area*. EAGE Publications b.v.

Dybkjaer, K., & Rasmussen, E. S. (2000). Palynological dating of the Oligocene–Miocene successions in the Lille Bælt area, Denmark. *Bulletin of the Geological Society of Denmark*, *47*, 87–103.

Dybkjær, K., Rasmussen, E. S., Eidvin, T., Grosfjeld, K., Riis, F., Piasecki, S., & Sliwinksa, K. K. (2021). A new stratigraphic framework for the Miocene – Lower Pliocene deposits offshore Scandinavia: A multiscale approach. *Geological Journal*, *56*(3), 1699–1725.

Eidvin, T., & Rundberg, Y. (2007). Post-Eocene strata of the southern Viking Graben, northern North Sea; intergrated biostratigraphic, strontium isotopic and lithostratigraphic study. *Norwegian Journal of Geology*, *87*, 391–450.

Everaert, S., Munsterman, D. K., De Schutter, P., Bosselaers, M., Van Boeckel, J., Cleemput, G., & Bor, T. (2020). Stratigraphy and palaeontology of the lower Miocene Kiel Sand Member (Berchem Formation) in temporary exposures in Antwerp (northern Belgium). *Geologica Belgica*, *23*, 167–198.

Flower, B. P., & Kennett, J. P. (1994). The middle Miocene climatic transition: East Antarctic ice sheet development, deep ocean circulation and global carbon cycling. *Palaeogeography, Palaeoclimatology, Palaeoecology*, *108*(3), 537–555.

Geluk, M. C., Duin, E. J. T., & Van den Berg, M. W. (1994). Stratigraphy and tectonics of the Roer Valley Graben. *Netherlands Journal of Geosciences – Geologie en Mijnbouw*, *73*, 129–141.

Gibbard, P., & Lewin, J. (2003). The history of the major rivers of southern Britain during the Tertiary. *Journal of the Geological Society*, *160*, 829–845.

Goledowski, B., Nielsen, S. B., & Clausen, O. R. (2012). Cenozoic erosion and flexural isostasy of Scandinavia. *Journal of Geodynamics*, *70*, 2813.

Hampson, G. J., Sixsmith, P. J., Kieft, R. L., Jackson, C. A.-L., & Johnson, H. D. (2009). Quantitative analysis of net-transgressive shoreline trajectories and stratigraphic architectures: Mid-to -late Jurassic of the North Sea Rift Basin. *Basin Research*, *21*, 528–558.

Haq, B. U., Hardenbol, J., & Vail, P. R. (1987). Chronology of Fluctuating Sea levels since the Triassic. *Science*, *235*(4793), 1156–1167.

Hardenbol, J., Thierry, J., Farley, M. B., Jacquin, T., de Graciansky, P.-C., & Vail, P. R. (1998). Mesozoic and Cenozoic sequence chronostratigraphic framework of European Basins. In P. C. de Graciansky, J. Hardenbol, T. Jacquin, & P. R. Vail (Eds.), *Mesozoic and Cenozoic sequence stratigraphy of European Basins* (Vol. *60*, pp. 3–29). SEPM Society for Sedimentary Geology.

Harding, R. (2015). *Evolution of the giant southern North Sea shelf-prism: testing sequence stratigraphic concepts and the global sea level curve with full-three dimensional control*. p. 296.

Helland-Hansen, W., & Hampson, G. J. (2009). Trajectory analysis: Concepts and applications. *Basin Research*, *21*(5), 454–483.

Helland-Hansen, W., & Martinsen, O. J. (1996). Shoreline trajectories and sequences: Description of variable depositional dip scenarios. *Journal of Sedimentary Research*, *B66*, 670–688.

Holbourn, A. E., Kuhnt, W., Clemens, S. C., Prell, W. L., & Andersen, N. (2013). Middle to late Miocene stepwise climate cooling: Evidence from a high-resolution deep water isotope curve spanning 8 million years. *Paleoceanography*, *28*(4), 688–699.

Houtgast, R. F., & van Balen, R. T. (2000). Neotectonics of the Roer Valley Rift System, the Netherlands. *Global and Planetary Change*, *27*, 107–123.

Houthuys, R. (2011). A sedimentary model of the Brussels Sands. *Eocene, Belgium, Geologica Belgica*, *14*(1–2), 55–74.

Houthuys, R. (2014). A reinterpretation of the Neogene emersion of central Belgium based on the sedimentary environment of the Diest Formation and the origin of the drainage pattern. *Geologica Belgica*, *17*(3–4), 211–235.

Houthuys, R., Adriaens, R., Goolaerts, S., Laga, P., Louwye, S., Matthijs, J., Vandenberghe, N., & Verhaegen, J. (2020). The diest formation: A review of insights from the last decades. *Geologica Belgica*, *23*(3–4), 1–20.

Hultberg, S. U., & Malmgren, B. A. (1986). Dinoflagellate and planktonic foraminiferal paleobathymetrical indices in the boreal uppermost Cretaceous. *Micropaleontology*, *32*, 316–323.

Huuse, M. (2002). Cenozoic uplift and denudation of southern Norway: Insights from the North Sea Basin. *Geological Society, London, Special Publications*, *196*(1), 209–233.

Huuse, M., & Clausen, O. R. (2001). Morphology and origin of major Cenozoic sequence boundaries in the eastern North Sea Basin: Top Eocene, near-top Oligocene and the mid-Miocene unconformity. *Basin Research*, *13*(1), 17–41.

Knox, R. W. O., Bosch, A., Hiss, M., De Lugt, I., Kasinski, J., King, C., Kothe, A., Slodkowska, B., Standke, G., & Vandenberghe, N. (2010). Cenozoic. In *Petroleum Geological Atlas of the Southern Permian Basin* (pp. 211–223). EAGE Publications b.v.

Kominz, M. A., Browning, J. V., Miller, K. G., Sugarman, P. J., Mizintseva, S., & Scotese, C. R. (2008). Late Cretaceous to Miocene sea-level estimates from the New Jersey and Delaware coastal plain coreholes: An error analysis. *Basin Research*, *20*(2), 211–226.

Louwye, S. (1999). New species of organic-walled dinoflagellates and acritarchs from the Upper Miocene Diest Formation, northern Belgium (southern North Sea Basin). *Review of Palaeobotany and Palynology*, *107*(1), 109–123.

Louwye, S. (2002). Dinoflagellate cyst biostratigraphy of the Upper Miocene Deurne Sands (Diest Formation) of northern Belgium, southern North Sea Basin. *Geological Journal*, *37*(1), 55–67.

Louwye, S. (2005). The Early and Middle Miocene transgression at the southern border of the North Sea Basin (northern Belgium). *Geological Journal*, *40*(4), 441–456.

Louwye, S., De Schepper, S., Laga, P., & Vandenberghe, N. (2007). The Upper Miocene of the southern North Sea Basin (northern Belgium): A palaeoenvironmental and stratigraphical reconstruction using dinoflagellate cysts. *Geological Magazine*, *144*(1), 33–52.

Louwye, S., Deckers, J., Verhaegen, J., Adriaens, R., & Vandenberghe, N. (2020). A review of the lower and middle Miocene of northern Belgium. *Geologica Belgica*, *23*, 137–156.

Meyer, W., Albers, H. J., Berners, H. P., Gehlen, K. V., Glatthaar, D., Lohnertz, W., Pfeffer, K. H., Schnutgen, A., Wienecke, K., & Zakosek, H. (1983). Pre-Quaternary uplift in the central part of the Rhenish Massif BT. In K. Y. Fuchs, K. Gehlen, H. Malzer, H. Muawski, & A. Semmel (Eds.), *Plateau uplift* (pp. 39–46). Springer Berlin Heidelberg.

Michon, L., & van Balen, R. T. (2005). Characterization and quantification of active faulting in the Roer valley rift system based on high precision digital elevation models. *Quaternary Science Reviews*, *24*(3–4), 457–474.

Michon, L., Van Balen, R. T., Merle, O., & Pagnier, H. (2003). The Cenozoic evolution of the Roer Valley Rift System integrated at a European scale. *Tectonophysics*, *367*(1), 101–126.

Miller, K. G., Browing, J. V., Schmelz, W. J., Kopp, R. E., Mountain, G. S., & Wright, J. D. (2020). Cenozoic sea-level and cryospheric evolution from deep-sea geochemical and continental margin records. *Science Advances*, *6*(20), eaaz1346.

Miller, K. G., Kominz, M. A., Browning, J. V., Wright, J. D., Mountain, G. S., Katz, M. E., Sugarman, P. J., Cramer, B. S., Christie-Blick, N., & Pekar, S. F. (2005). The Phanerozoic Record of global sea-level change. *Science*, *310*(5752), 1293–1298.

Munsterman, D. K., & Brinkhuis, H. (2004). A southern North Sea Miocene dinoflagellate cyst zonation. *Netherlands Journal of Geosciences – Geologie en Mijnbouw*, *83*(4), 267–285.

Munsterman, D. K., & Deckers, J. (2020). The Oligocene/Miocene boundary in the ON-Mol-1 and Weelde boreholes along the southern margin of the North Sea Basin, Belgium. *Geologica Belgica*, *23*(3–4), 127–135.

Munsterman, D. K., & Deckers, J. (2022). Biostratigraphic ages and depositional environments of the upper Oligocene to lower Miocene Veldhoven Formation in the central Roer Valley Rift System (SE Netherlands-NE Belgium). *Netherlands Journal of Geosciences – Geologie en Mijnbouw*, *101*, 6.

Munsterman, D. K., Ten Veen, J. H., Menkovic, A., Deckers, J., Witmans, N., Verhaegen, J., Kerstholt-Boegehold, S. J., Van de Ven, T., & Busschers, F. S. (2019). An updated and revised stratigraphic framework for the Miocene and earliest Pliocene strata of the Roer Valley Graben and adjacent blocks. *Geologie en Mijnbouw/Netherlands Journal of Geosciences*, *98*, 1993–1997.

Ogg, J., Ogg, G., & Gradstein, F. (2016). *A Concise Geologic TimeScale 2016*. Elsevier.

Patruno, S., Hampson, G. J., Jackson, C. A. L., & Dreyer, T. (2015). Clinoform geometry, geomorphology, facies character and stratigraphic architecture of a sand-rich subaqueous delta: Jurassic Sognefjord Formation, offshore Norway. *Sedimentology*, *62*(1), 350–388.

Patruno, S., & Helland-Hansen, W. (2018). Clinoforms and clinoform systems: Review and dynamic classification scheme for shorelines, subaqueous deltas, shelf edges and continental margins. *Earth-Science Reviews*, *185*, 202–233.

Posamentier, H. W., Jervey, M. T., & Vail, P. R. (1988). Eustatic controls on clastics deposition I—Conceptual framework. In C. K. Wilgus, B. H. Hasting, C. G. S. T. C. Kendall, H. W. Posamentier, C. A. Ross, & J. C. van Wagoner (Eds.), *Sea level changes: An integrated approach* (pp. 109–124). SEPM, Special Publication, No. 420.

Prinz, L., McCann, T., Schäfer, A., & Asmus, S. (2016). The geometry, distribution and development of sand bodies in the Miocene-age Frimmersdorf Seam (Garzweiler open-cast mine), Lower Rhine Basin, Germany: Implications for seam exploitation. *Geological Magazine*, *155*(3), 685–706.

Prinz, L., Schäfer, A., McCann, T., Utescher, T., Lokay, P., & Asmus, S. (2017). Facies analysis and depositional model of the Serravallian-age Neurath Sand, Lower Rhine Basin (W Germany). *Netherlands Journal of Geosciences – Geologie en Mijnbouw*, *96*(3), 211–231.

Rasmussen, E. S. (2014). Development of an incised-valley fill under the influence of tectonism and glacio-eustatic sea-level change: Valley morphology, fluvial style, and lithology. *Journal of Sedimentary Research*, *84*(4), 278–300.

Rasmussen, E. S., & Dybkjær, K. (2014). Patterns of Cenozoic sediment flux from western Scandinavia: Discussion. *Basin Research*, *26*(2), 338–346.

Rasmussen, E. S., Dybkjær, K., & Piasecki, S. (2010). Lithostratigraphy of the upper Oligocene – Miocene succession of Denmark. *Bulletin of the Geological Survey of Denmark and Greenland*, *22*, 1–92.

Rasmussen, E. S., Heilmann-Clausen, C., Waagstein, R., & Eidvin, T. (2008). Tertiary of Norden. *Episodes*, *31*, 66–72.

Schäfer, A., Utescher, T., Klett, M., & Manchego, M. V. (2005). The Cenozoic Lower Rhine Basin – Rifting, sedimentation, and cyclic stratigraphy. *International Journal of Earth Sciences*, *94*(4), 621–639.

Shevenell, A. E., Kennett, J. P., & Lea, D. W. (2008). Middle Miocene ice sheet dynamics, deep-sea temperatures, and carbon cycling: A Southern Ocean perspective. *Geochemistry, Geophysics, Geosystems*, *9*(2), Q02006.

Sissingh, W. (2003). Tertiary paleogeographic and tectonostratigraphic evolution of the Rhenish Triple Junction. *Palaeogeography, Palaeoclimatology, Palaeoecology*, *196*, 229–263.

Slupik, A., & Janse, A. C. (2008). *The geological record of the Breda Formation in the subsurface of the Island of Noord-Beveland (Province of Zeeland, The Netherlands) from the Colijnsplaat borehole (42G24-1): A sequence-stratigraphic approach*. Deinsea.

Sørensen, J. C., Gregersen, U., Breiner, M., & Michelsen, O. (1997). High-frequency sequence stratigraphy of Upper Cenozoic deposits in the central and southeastern North Sea areas. *Marine and Petroleum Geology*, *14*(2), 99–123.

Steel, R., Porebski, S. J., Plink-Bjorklund, P., & Mellere, D. (2003). Shelf-edge delta types and their sequence-stratigraphic relationships. *Shelf Margin Deltas and Linked Down Slope Petroleum Systems: 23rd Annual*, 205–230.

Steel, R. J., & Olsen, T. (2002). Clinoforms, clinoform trajectory and deepwater sands. In J. M. Armentrout & N. C. Rosen (Eds.), *Sequence stratigraphic models for exploration and production: Evolving methodology, emerging models and application histories* (pp. 367–381). GCS-SEPM Special Publication.

Thöle, H., Gaedicke, C., Kuhlmann, G., & Reinhardt, L. (2014). Late Cenozoic sedimentary evolution of the German North Sea – A seismic stratigraphic approach. *Newsletters on Stratigraphy*, *47*(3), 299–329.

TNO-GDN. (2024). *Stratigraphic nomenclature of the Netherlands*. TNO—Geological Survey of the Netherlands. https://www.dinoloket.nl/en/stratigraphic-nomenclature

Utescher, T., Ashraf, A., Kern, A. K., & Mosbruger, V. (2021). Diversity patterns in microfloras recovered from Miocene brown coals of the lower Rhine Basin reveal distinct coupling of the structure of the peat-forming vegetation and continental climate variability. *Geological Journal*, *56*(2), 768–785.

Utescher, T., Mosbrugger, V., & Ashraf, A. (2000). Terrestrial climate evolution in Northwest Germany over the last 25 million years. *PALAIOS*, *15*, 430–449.

Utescher, T., Mosbrugger, V., & Ashraf, A. R. (2002). Facies and paleogeography of the Tertiary of the Lower Rhine Basin—sedimentary versus climatic control. *Netherlands Journal of Geosciences – Geologie en Mijnbouw*, *81*(2), 185–191.

Van Adrichem Boogaert, H. A., & Kouwe, W. F. P. (1993). Stratigraphic nomenclature of the Netherlands; revision and update by RGD and NOGEPA. *Mededelingen Rijks Geologische Dienst*, *50*, 1–39.

Van Balen, R. T., Verweij, J. M., Van Wees, J. D. A. M., Simmelink, H., Van Bergen, F., & Pagnier, H. (2002). Deep subsurface temperatures in the Roer Valley Graben and the Peelhorst, the Netherlands-new results. *Netherlands Journal of Geosciences – Geologie en Mijnbouw*, *81*, 19–26.

Vandenberghe, N., Burleigh Harris, W., Wampler, J. M., Houthuys, R., Louwye, S., Adriaens, R., Vos, K., Lanckacker, T., Matthijs, J., & Deckers, J. (2014). The implications of K-Ar glauconite dating of the diest formation on the paleogeography of the upper miocene in Belgium. *Geologica Belgica*, *17*(2), 161–174.

Vandenberghe, N., Laga, P., Louwye, S., Vanhoorne, R., Marquet, R., De Meuter, F., Wouters, K., & Hagemann, H. W. (2005). Stratigraphic interpretation of the Neogene marine-continental record in the Maaseik well (49W0220) in the Roer Valley Graben, NE Belgium. *Memoirs of the Geological Survey of Belgium*, *52*, 39.

Vandenberghe, N., Laga, P., Steurbaut, E., Hardenbol, J., & Vail, P. R. (1998). Tertiary sequence stratigraphy at the southern border of the North Sea Basin in Belgium. *Mesozoic and Cenozoic Sequence Stratigraphy of European Basins*, *60*, 119–154.

Verbeek, J. W., de Leeuw, C. S., Parker, N., & Wong, T. E. (2002). Characterisation and correlation of Tertiary seismostratigraphic units in the Roer Valley Graben. *Netherlands Journal of Geosciences – Geologie en Mijnbouw*, *81*(2), 159–166.

Wang, R., Colombera, L., & Mountney, N. P. (2020). Quantitative analysis of the stratigraphic architecture of incised-valley fills: A global comparison of Quaternary systems. *Earth-Science Reviews*, *200*, 102988.

Westerhoff, W. E., Kemna, H. A., & Boenigk, W. (2008). The confluence area of Rhine, Meuse, and Belgian rivers: Late Pliocene and Early Pleistocene fluvial history of the northern Lower Rhine Embayment. *Netherlands Journal of Geosciences – Geologie en Mijnbouw*, *87*(1), 107–125.

Whitcombe, D. N. (2002). Extended elastic impedance for fluid and lithology predication. *Geophysics*, *67*, 63–67.

Wong, T. E., Parker, N., & Horst, P. (2001). Tertiary sedimentary development of the Broad Fourteens area, the Netherlands. *Netherlands Journal of Geosciences – Geologie en Mijnbouw*, *80*(1), 85–94.

Zagwijn, W. H., & Hager, H. (1987). Correlations of continental and marine Neogene deposits in the south-eastern Netherlands and the Lower Rhine District. *Medewerkers Werkgroep Tertair Kwartair Geologie*, *24*(1–2), 59–78.

Ziegler, P. A. (1990). *Geological atlas of western and central Europe* (2nd ed.). Shell Internationale Petroleum Maatschappij.

Ziegler, P. A. (1994). Cenozoic rift system of western and central Europe: An overview. *Netherlands Journal of Geosciences – Geologie en Mijnbouw*, *73*(2–4), 99–127.

How to cite this article: Siebels, A., ten Veen, J., Munsterman, D., Deckers, J., Kasse, C., & van Balen, R. (2024). Miocene sequences and depocentres in the Roer Valley Rift System. *Basin Research*, *36*, e12886. https://doi.org/10.1111/bre.12886